Quaternary International 516 (2019) 21–41

Contents lists available at ScienceDirect

Quaternary International

journal homepage: www.elsevier.com/locate/quaint

Postglacial vegetation and climate history and traces of early human impact and agriculture in the present-day cool mixed forest zone of European Russia

Pavel E. Tarasov [a, *], Larisa A. Savelieva [b], Tengwen Long [a, c], Christian Leipe [a]

[a] Institute of Geological Sciences, Palaeontology Section, Free University of Berlin, Malteserstr. 74-100, Building D, 12249 Berlin, Germany
[b] Institute of Earth Sciences, St. Petersburg State University, Russia
[c] Eurasia Department, German Archaeological Institute, Berlin, Germany

ARTICLE INFO

Article history:
Received 10 December 2017
Received in revised form
9 February 2018
Accepted 21 February 2018
Available online 6 March 2018

Keywords:
Lateglacial
Holocene
Neolithic
Cereal pollen
Radiocarbon chronology
Bayesian age model

ABSTRACT

This study is based on the reassessment and correlation of five pollen records from the upper Western Dvina River region. For the most complete record (Korovinskoe Mire; 56°16′N, 31°20′E) we constructed a Bayesian age-depth model to provide robust chronological control for the reconstructed changes in the regional environments and to facilitate interregional comparisons. The results show that the Holocene Thermal Maximum in the study region (ca. 8600–6900 cal BP) started and ended some centuries earlier than suggested for the neighboring Baltic region (ca. 8100–5600 cal BP). The spruce (*Picea*) pollen records corroborate other palaeobotanical records from the wider region indicating a relatively dry early and middle Holocene and cooler/wetter conditions after ca. 5400 cal BP. Local initial opening of forests by Neolithic populations is indicated by 7600 cal BP and a stepwise intensification of forest clearance is registered from ca. 4200/3700 and ca. 1400–1000 cal BP. There is evidence for an asynchronous pattern of human impact during the early period of occupation prior to ca. 4000 cal BP, which can be explained by a low density and uneven distribution of prehistoric hunter-fisher-gatherer populations. Although single *Cerealia*-type pollen grains are registered as early as ca. 6700 cal BP, intensive cultivation of cereals in the study region probably did not occur before ca. 1400 cal BP, i.e. much later than suggested for the Baltic states, Poland, and Belarus.

1. Introduction

Pollen-based reconstructions of vegetation and climate changes and spread of agriculture across the globe during the Holocene have been traditionally among the topics most frequently addressed and lively debated by geoscientists and archaeologists (e.g. An et al., 2010; Jones et al., 2012; Spengler et al., 2016). In the recent decades, the aforesaid research problematic got a new impulse due to growing interest in the results from the scientific community dealing with Earth-system and land cover modeling (e.g. Gaillard et al., 2010; d'Alpoim Guedes, 2016).

Central European Russia (CER) between ca. 54 and 58°N represents the most densely populated part of the country with an economy based on developed industry and intensive agriculture. The first Holocene pollen records from this region were reported by I.P. Gerasimov, V.S. Dokturovskii, M.I. Neishtadt, and some others already in the early 1920s, i.e. soon after the introduction of pollen analysis hundred years ago (for a detailed overview of these early works and references see Grichuk and Zaklinskaya (1948) and Neishtadt (1957)). A new phase of intensive palynological research on Holocene peat and lake sediments from CER occurred in the late 1960s and 1970s with a focus on millennial-scale vegetation changes and human occupation in the region (e.g. Khotinsky, 1977 and references therein). Results of palynological studies obtained during this period for the first time were accompanied with absolute age determinations by the radiocarbon dating method. Summarizing available pollen and radiocarbon data from the USSR territory, Khotinsky (1977) made an attempt to reconstruct the vegetation and climate history of Northern Eurasia since ca. 12,000 ^{14}C years before present (^{14}C BP), i.e. of the Lateglacial–Holocene interval. Among the achievements of this work (Khotinsky, 1977)

* Corresponding author.
E-mail addresses: ptarasov@zedat.fu-berlin.de (P.E. Tarasov), savelieval@mail.ru (L.A. Savelieva), longtengwen@zedat.fu-berlin.de (T. Long), c.leipe@fu-berlin.de (C. Leipe).

https://doi.org/10.1016/j.quaint.2018.02.029
1040-6182/

is a comprehensive chart presenting reconstructed trends in temperature and precipitation over the CER region along with major changes in the regional pollen assemblages and vegetation composition. Merely based on five unequally dated pollen records of multi-centennial resolution, this regional scheme, however, became a powerful tool for pollen-based correlations and palaeoenvironmental interpretations during the following decades (e.g. Klimanov, 1984; Khotinsky and Klimanov, 1997; Velichko et al., 1997; Krementski et al., 2000; Zernitskaya and Mikhailov, 2009; Novenko et al., 2015). Regrettably, the research trend towards the higher-resolution and better-dated pollen archives from the CER region did not continue during the 1980s and 1990s. The collapse of the Soviet Union intensified the level of international cooperation resulting in the appearance of new high-resolution and better-dated pollen records from Siberia, the Russian Far East, and the Arctic (Andreev and Tarasov, 2013). By contrast, the interest in the cool temperate zone of European Russia and publications of new records remained rather sporadic (e.g. Wohlfarth et al., 2007; Gunova et al., 2001; Novenko et al., 2009, 2015).

This article presents five pollen records representing extensively radiocarbon dated sediment cores collected within a small area in the upper reaches of the Western Dvina River within the CER region (Fig. 1) and their interpretations in terms of post-glacial vegetation history, palaeoclimate, early agriculture, and human land use. The core sediments were intensively studied and the results of the radiocarbon dating and peat composition, diatom and pollen analyses were partly presented in several papers and non-peer-reviewed monographs (Dolukhanov et al., 2004; Arslanov et al., 2009; Mazurkevich et al., 2012) and in Russian sources poorly accessible for the international readership. None of the previous publications presents a comprehensive summary of the regional pollen data illustrated by pollen diagrams of good quality. This gap is filled by the current paper aiming at reconstructing the vegetation and climate dynamics in the study region since the Lateglacial and discussing traces of human impact and agriculture in the pollen diagrams. For the first time in the CER region, a Bayesian age modeling approach is applied to the numerous radiocarbon dates in attempt to build a robust age-depth model for the analyzed pollen records and to allow comprehensive inter-regional comparisons with archaeological and environmental records elsewhere. Our paper attempts to address the following questions including: (1) whether the investigated pollen records from the western part of CER can be satisfactorily correlated with each other and with the reference pollen profile from the central part of the region; (2) what is the earliest pollen-based evidence for human impact and agriculture in the study region and does it corroborate the archaeological evidence; and (3) whether timing of the Holocene Thermal Maximum (HTM) in the study region indicated by the pollen percentages of thermophilous tree taxa support the diachronous pattern of temperature change suggested by climate reconstructions from the Norwegian Sea and the eastern Baltic region.

2. Regional setting and environments

Our study area (Fig. 1) occupies the western part of the CER region. The study sites are located in the central part of the East European Plain – a vast interior plain extending roughly from 25°E eastward and comprising several elevated plains and hills including the Central Russian Upland, the Smolensk-Moscow Upland, and the Valdai Hills (Fig. 1). While average elevations vary between 100 and 250 m a.s.l., the highest point of the plain (347 m a.s.l.) is located in the Valdai Hills, where major rivers including the Volga, Western Dvina, Dnieper, and Lovat have their origin. The region thus is divided between the drainage basins of the Caspian Sea, the Black Sea, and the Baltic Sea (Alpat'ev et al., 1976).

The study sites presented in the current paper (Fig. 1) are all located in the upper reaches of the Western Dvina River, which is also called Zapadnaya Dvina in Russia and Daugava in Latvia. The river originates in the Valdai Hills, flows westward into the Gulf of Riga, and crosses, on its way to the Baltic Sea, the Western Dvina Lowland (*Zapadnodvinskaya Nizina*) bordered by the Smolensk-Moscow Upland in the south. While the uplands are composed of dolomite, limestone, and clay dating to the Palaeozoic and strongly modified by the glacial and fluvial processes during the Middle and Late Pleistocene, the low-elevated parts consist of numerous topographic depressions of glacial, fluvial, and fluvioglacial origin recently occupied by lakes and peat mires (see Alpat'ev et al. (1976) and Dolukhanov et al. (2009) for a detailed overview).

The modern climate of the study region is moderately continental and experiences a pronounced influence of Atlantic air masses throughout the year (Alpat'ev et al., 1976). Summers are moderately cool and humid. About 60% of the annual precipitation falls in May to October, while winters are long and moderately cold with a stable snow cover trough November to April. The weather and climate data from the Smolensk Meteorological Observatory (54°46′58″N; 32°02′43″E) reveal a warmest summer month (July) average temperature of 17.8 °C and an average temperature of the coldest month (February) of −6.4 °C. The annual temperature and atmospheric precipitation averages are 5.4 °C and 738 mm, respectively (Weather and climate, 2016). However, the amount of precipitation may vary significantly from year to year, i.e. from 366 mm in 1951 to 1030 mm in 1998.

Forests with a dominance of boreal summergreen broadleaf trees (e.g. birch, alder, and aspen) and evergreen conifers (e.g. spruce and Scots pine) dominate in the natural vegetation cover. *Sphagnum* peat bogs occupy swampy depressions and lowland areas. Well-drained higher-elevated sites with more favourable thermal conditions may host temperate deciduous broadleaf trees and shrubs such as hazel (*Corylus*), linden (*Tilia*), elm (*Ulmus*), maple (*Acer*), oak (*Quercus*), and ash (*Fraxinus*), which are representatives of cool conifer (southern taiga) and cool mixed forests (see Prentice et al., 1992, 1996 for definition of the major regional biomes and their bioclimatic ranges).

3. Data and methods

3.1. Coring and lithology

Coring of peat layers and underlying lacustrine sediment was performed manually using a so-called Russian peat corer with a one-meter long sampler (see Dolukhanov et al., 2009 for details of the fieldwork). The sampler with an inner diameter of 7.5 cm was applied to the soft peat and gyttja layers and the sampler with a 5-cm diameter was used for coring of the deeper and viscous mud and clay layers. The recovered cores were sub-sampled in the field and 5-cm segments wrapped in plastic film were transported to the pollen laboratory at St. Petersburg State University, where they were stored at cool temperature for further analyses. Core lithology and sediment stratigraphy were first described in the field and further refined in the laboratory. Individual overlapping core segments were correlated using characteristic marker horizons in the laboratory. Lithological descriptions of the cores discussed in the current study are presented in Table 1.

3.2. Radiocarbon dating and chronology

A total of 178 bulk sediment samples were selected from the five sequences and radiocarbon dated using the conventional approach (Table 2). Bulk organic samples taken for radiocarbon dating were

Fig. 1. Map showing regional topographic features and modern hydrology. Locations of main cities and modern state boundaries are provided for orientation. The white square indicates the study area in the upper Western Dvina River region. The white circles indicate study site locations (K – Korovinskoe, P – Prigorodnoe, S – Serteika, S2 – Serteya 2, Z – Zmeinoe). Other study sites discussed in the text are signed and marked by black circles.

processed in the Radiocarbon Laboratory of St. Petersburg State University. Measurement and calculation of radiocarbon dates followed techniques described in Arslanov (1993) and Muraki et al. (2001). Calibrated ages (i.e. cal BP: Table 2; Fig. 2) were obtained using OxCal v4.2 (Bronk Ramsey, 1995). IntCal13 (Reimer et al., 2013) and Bomb13NH1 (Hua et al., 2013) calibration curves were used for prebomb and postbomb dates, respectively (see Demske et al., 2016 for the technical details). Age-depth relationships were modeled in BACON v2.2 (Blaauw and Christen, 2011) on the R v.3.2.4 platform (R Core Team, 2016). BACON aims specifically at modeling lacustrine and palustrine (e.g. peat and mire) sequences by using Bayesian methods and is recognized as a standard chronological package for such environments (e.g. Payne et al., 2016). Priors were set following recommended values in Goring et al. (2012), which were found applicable for the studied region (see Payne et al., 2016).

3.3. Pollen analysis and presentation of results

Samples for palynological investigations were taken from the cores at 5–10 cm intervals and prepared using standard techniques (Grichuk and Zaklinskaya, 1948; Fægri and Iversen, 1989). Pollen

Table 1
Simplified lithological description of Korovinskoe, Prigorodnoe, Serteika, Serteya 2, and Zmeinoe sediment cores presented in the current study.

Site name	Core depth (cm)	Sediment
Korovinskoe	0–100	Peat rich in plant macrofossils
	100–240	Dark–brown well decomposed peat with wood macrofossils at 165–170 cm and 180–190 cm depth
	240–440	Black peat
	440–500	Olive gyttja with white carbonaceous spots
	500–740	Olive gyttja
	740–780	Black gyttja
	780–830	Laminated black gyttja with clay layers
	830–840	Clay
	840–850	Sandy clay
Prigorodnoe	0–230	Light–brown poorly decomposed sphagnum peat
	230–577	Dark–brown peat. High water content at 230–250 cm depth
	577–580	Transitional layer
	580–640	Olive gyttja with rich in organics
	640–686	Brown gyttja
	686–710	Clayey gyttja
	710–820	Gyttja with admixture of sand and lack of plant macrofossils
	820–833	Gyttja with admixture of sand and plant macrofossils
	833–840	Laminated clayey gyttja
	840–850	Grey silt with few plant macrofossils
Serteika	0–15	Peat
	15–73	Dense dark brown gyttja
	73–320	Brown gyttja with abundant plant macrofossils, including small wood particles. Remains of small (non-identified) fresh-water shells at 133 cm depth
	320–695	Olive gyttja
	695–750	Dense black gyttja
	750–850	Clayey silt
Serteya 2	0–50	Peat
	50–60	Transitional layer
	60–100	Gyttja with plant macrofossils
	100–150	Gyttja, archaeologically identified as cultural layer of “pile dwelling” epoch
	150–190	Gyttja with plant macrofossils, including wood particles.
	190–260	Olive gyttja. Nuts of *Trapa natans* at 242 cm depth
	260–280	Clayey gyttja with remains of small (non-identified) fresh-water shells
	200–460	Dense clayey gyttja
Zmeinoe	0–150	Dark–brown peat with plant macrofossils
	150–340	Dark–brown well decomposed peat
	340–362	Brown peat with admixture of olive gyttja
	362–419	Olive gyttja
	419–431	Sandy silt
	431–450	Laminated blue clay

and spore identification was carried out using published references and the reference collections at St. Petersburg State University. In each sample between 400 and 600 terrestrial pollen grains were counted. The basic pollen sum includes terrestrial arboreal pollen (AP) and non-arboreal pollen (NAP) taxa excluding counts of aquatic taxa and non-pollen palynomorphs (e.g. fern, moss, and green algae spores). Individual taxa percentages were calculated based upon the total sum of arboreal and non-arboreal pollen (AP and NAP) taken as 100%. The Tilia software package, including Tilia 2.0.b.4, TiliaGraph 2.0.b.5, and TiliaGraphView 1.0.7.2 (Grimm, 1990, 2000), was used for calculating taxa percentages and constructing pollen diagrams. The subdivision into local pollen assemblage zones (LPAZ) was facilitated using the CONISS program for stratigraphically constrained cluster analysis (Grimm, 1987) integrated in the Tilia package. Additionally, regional chronostratigraphic boundaries were drawn following the classic scheme proposed by Khotinsky (1977, 1980). This scheme has been regarded as the standard for the entire CER region, although it was primarily constructed using the pollen analysis results and the age-model based on 14 uncalibrated radiocarbon dates of bulk peat and gyttja sediments from the stratotype section Polovetsko-Kupanskoe (~57°N, ~39°E; Fig. 1) in the Yaroslavl region (Khotinsky, 1977; Khotinsky and Klimanov, 1997), ca. 450 km east of the sites presented in our current study.

4. Results and interpretations

4.1. Changes in the local pollen assemblages and vegetation

4.1.1. Korovinskoe Mire

This chapter provides short descriptions of the pollen records shown in Figs. 3-6. All LPAZs are consequently numbered from the top to the bottom of each record. The Korovinskoe pollen diagram (Fig. 3) is divided into seven major pollen zones. To facilitate further interpretation and discussion, the key features of the pollen assemblage zones are provided starting from the bottom one.

LPAZ Ko-7 (775–850 cm) reveals relatively low AP percentages (58–76%), mainly boreal deciduous and coniferous taxa (*Betula* sect. *Albae*, *Picea*, and *Pinus*). Shrubby forms of birch (*Betula* sect. *Nanae* + *Fruticosae*) and possibly of alder (*Alnus*) reach respectively 15% and 10% in the bottommost spectra, accompanied with the highest contents of *Picea* (up to 30%), *Artemisia* (ca. 15%), Poaceae (up to 20%), and Chenopodiaceae (up to 5%). In the upper part of this zone, higher values of *Pinus* (up to 40%) and *Betula* sect. *Albae* (30–40%) are registered accompanied by lower values of birch shrubs and *Artemisia* (5–10%), and virtual disappearance of Chenopodiaceae pollen. The pollen assemblage composition suggests semi-open landscape with forest patches containing spruce, birch, and pine occupying the river valleys and sandy terraces. Shrubby

Table 2
Radiocarbon dating results obtained on bulk sediments from Korovinskoe, Prigorodnoe, Serteika, Serteya 2, and Zmeinoe along with the respective calibrated ages expressed as 95% probability ranges and median point estimates. The radiocarbon datings (^{14}C BP) were calibrated using OxCal v.4.2 software. The two uppermost dates (LU-4853 and LU-4852) in the Prigorodnoe Peat are reported with their F^{14}C values (according to Reimer et al., 2004) and calibrated with Bomb13NH1 calibration curve (Hua et al., 2013). All other dates are reported with their radiocarbon age and calibrated using IntCal13 calibration curve (Reimer et al., 2013).

Site name and radiocarbon laboratory code	Core depth (cm)	Radiocarbon date (^{14}C BP)	Calibrated age, 95% range (cal BP)	Calibrated age, Median (cal BP)
Korovinskoe				
LU-4957	10–20	330 ± 60	505–289	392
LU-4955	30–40	480 ± 60	646–326	518
LU-4951	70–80	1200 ± 70	1275–976	1126
LU-4949	90–100	1710 ± 80	1820–1415	1626
LU-4947	110–120	2310 ± 70	2694–2132	2330
LU-4945	130–140	2550 ± 50	2760–2469	2622
LU-4943	150–160	2900 ± 50	3176–2881	3038
LU-4939	170–180	3270 ± 80	3695–3345	3504
LU-4937	190–200	3330 ± 70	3811–3395	3565
LU-4935	210–220	3480 ± 80	3971–3566	3754
LU-4933	230–240	3630 ± 80	4215–3710	3951
LU-4931	250–260	3640 ± 60	4149–3780	3962
LU-4927	290–300	4510 ± 60	5435–4966	5157
LU-4923	330–340	4670 ± 60	5583–5300	5409
LU-4999	340–350	4450 ± 70	5293–4875	5091
LU-5000	350–360	4400 ± 70	5285–4848	5007
LU-5001	360–370	4580 ± 60	5466–5046	5265
LU-5002	380–390	4670 ± 60	5583–5300	5409
LU-5003	400–410	5050 ± 80	5932–5611	5796
LU-5004	420–430	6010 ± 80	7156–6664	6858
LU-5005	440–450	6130 ± 70	7240–6799	7024
LU-5006	460–470	6250 ± 100	7417–6930	7158
LU-5007	470–480	6730 ± 90	7735–7434	7594
LU-5008	490–500	6850 ± 100	7929–7517	7700
LU-5009	520–530	7520 ± 100	8543–8067	8325
LU-5011	560–570	7800 ± 110	8979–8406	8615
LU-5017	570–580	8300 ± 90	9480–9032	9294
LU-5012	580–590	8450 ± 220	10172–8811	9438
LU-5018	590–600	8340 ± 80	9518–9126	9343
LU-5013	600–610	8510 ± 100	9736–9271	9502
LU-5019	610–620	8430 ± 110	9609–9094	9420
LU-5014	620–630	8590 ± 100	9907–9417	9592
LU-5020	630–640	8600 ± 110	10118–9329	9612
LU-5015	640–660	8920 ± 110	10251–9634	10004
LU-5016	660–670	8810 ± 110	10176–9561	9872
LU-5026	710–720	9960 ± 100	11918–11201	11466
LU-5027	720–740	10120 ± 120	12148–11256	11726
LU-5029	760–780	10260 ± 110	12521–11412	12016
LU-5030	780–800	10250 ± 200	12565–11292	11972
LU-5032	830–840	11140 ± 180	13323–12707	12999
Prigorodnoe				
LU-4853	20–30	Postbomb F^{14}C: 1.1084 ± 0.0070	(-7)-(-50)	−47
LU-4852	30–40	Postbomb F^{14}C: 1.1450 ± 0.0007	(-7)-(-42)	−41
LU-4849	50–60	130 ± 40	281–6	133
LU-4848	70–80	300 ± 70	506–0	372
LU-4847	90–100	610 ± 50	665–536	601
LU-4846	100–110	800 ± 50	895–664	722
LU-4845	130–140	740 ± 50	764–563	684
LU-4844	150–160	840 ± 40	902–681	750
LU-4843	170–180	1020 ± 60	1059–792	935
LU-4842	190–200	1080 ± 70	1180–800	1003
LU-4841	210–220	1210 ± 60	1276–984	1137
LU-4840	230–240	1480 ± 60	1522–1295	1377
LU-4839	250–260	1790 ± 60	1865–1566	1715
LU-4838	270–280	2140 ± 60	2315–1990	2132
LU-4837	290–300	2340 ± 50	2686–2160	2368
LU-4836	310–320	2400 ± 60	2705–2339	2464
LU-4834	330–340	2670 ± 50	2874–2733	2787
LU-4833	340–350	2900 ± 60	3209–2872	3039
LU-4832	350–360	2930 ± 60	3320–2886	3080
LU-4831	360–370	3140 ± 60	3480–3182	3357
LU-4830	370–380	3250 ± 50	3583–3375	3478
LU-4829	380–390	3420 ± 60	3841–3509	3677
LU-4828	390–400	3560 ± 70	4081–3645	3854
LU-4827	400–410	3510 ± 60	3965–3636	3782
LU-4826	410–420	3640 ± 60	4149–3780	3962
LU-4825	420–430	3970 ± 60	4782–4237	4434

(continued on next page)

Table 2 (*continued*)

Site name and radiocarbon laboratory code	Core depth (cm)	Radiocarbon date (^{14}C BP)	Calibrated age, 95% range (cal BP)	Calibrated age, Median (cal BP)
LU-4822	450–460	4570 ± 70	5468–4979	5227
LU-4821	460–470	4550 ± 100	5571–4879	5194
LU-4817	480–490	4480 ± 60	5310–4887	5136
LU-4816	490–500	4980 ± 60	5892–5602	5716
LU-4814	500–510	4960 ± 70	5892–5590	5702
LU-4813	510–520	5200 ± 100	6266–5734	5974
LU-4806	520–530	5130 ± 60	5997–5726	5866
LU-4805	530–540	5310 ± 90	6280–5922	6094
LU-4803	550–560	5550 ± 60	6466–6216	6349
LU-4802	560–570	5560 ± 60	6475–6222	6355
LU-4801	570–580	5960 ± 60	6942–6665	6794
LU-4800	580–590	6410 ± 70	7439–7175	7340
LU-4798	600–610	7060 ± 110	8155–7672	7881
LU-4797	610–620	7350 ± 110	8374–7975	8169
LU-4796	620–630	7410 ± 120	8419–7983	8228
LU-4795	630–640	8100 ± 140	9413–8628	9022
LU-4794	640–660	8370 ± 120	9542–9033	9349
LU-4792	660–680	9200 ± 120	10709–10172	10393
LU-4790	680–700	9600 ± 170	11390–10421	10928
Serteika				
LU-4282	10–20	730 ± 70	789–551	678
LU-4281	20–35	690 ± 50	722–553	649
LU-4280	35–50	1170 ± 60	1259–961	1097
LU-4279	50–66	1110 ± 90	1264–802	1038
LU-4268	66–83	850 ± 50	908–682	765
LU-4267	83–100	1170 ± 50	1237–965	1096
LU-4266	100–116	1560 ± 70	1600–1311	1458
LU-4265	116–133	1560 ± 90	1690–1297	1461
LU-4264	133–150	1790 ± 70	1870–1560	1715
LU-4263	166–183	2150 ± 40	2307–2005	2145
LU-4261	183–200	2280 ± 66	2465–2120	2265
LU-4259	200–216	2250 ± 50	2348–2150	2237
LU-4260	216–233	2370 ± 50	2700–2312	2419
LU-4269	233–250	2310 ± 60	2677–2150	2328
LU-4270	250–266	2320 ± 60	2680–2153	2341
LU-4271	266–283	2490 ± 70	2739–2365	2568
LU-4272	283–300	2540 ± 60	2761–2381	2603
LU-4273	300–316	3560 ± 290	4808–3181	3901
LU-4274	316–333	5990 ± 120	7165–6550	6843
LU-4275	333–350	6060 ± 280	7476–6318	6927
LU-4276	350–366	7820 ± 180	9193–8217	8683
LU-4277	366–383	6680 ± 150	7839–7291	7558
LU-4278	383–400	7780 ± 250	9301–8056	8658
LU-4258	400–416	7060 ± 130	8164–7665	7883
LU-4257	416–433	7380 ± 130	8411–7962	8199
LU-4256	433–450	7510 ± 140	8580–8026	8313
LU-4255	450–466	7800 ± 120	8981–8405	8623
LU-4254	466–483	7580 ± 150	8716–8029	8388
LU-4252	500–516	8140 ± 130	9433–8652	9088
LU-4251	516–533	8730 ± 160	10199–9486	9800
LU-4250	533–550	8950 ± 170	10485–9556	10026
LU-4249	550–560	9090 ± 160	10674–9710	10254
LU-4248	560–583	8590 ± 150	10153–9290	9625
LU-4247	583–600	9520 ± 140	11215–10435	10850
LU-4246	600–616	10980 ± 250	13406–12405	12887
LU-4245	616–633	10530 ± 220	12846–11620	12362
LU-4244	633–650	9990 ± 150	12085–11169	11548
LU-4243	650–666	10750 ± 140	13011–12248	12667
LU-4242	666–683	11440 ± 230	13746–12821	13292
LU-4241	683–700	12000 ± 300	15028–13287	13968
Serteya 2				
LU-4888	10–20	470 ± 50	631–332	514
LU-4887	20–30	930 ± 60	955–729	844
LU-4886	30–40	1080 ± 50	1173–918	995
LU-4885	40–50	1480 ± 50	1521–1296	1371
LU-4884	50–60	2130 ± 60	2311–1952	2118
LU-4883	60–70	2820 ± 70	3142–2776	2935
LU-4882	70–80	2940 ± 70	3333–2885	3095
LU-4881	80–90	3050 ± 80	3444–3005	3244
LU-4880	90–100	3180 ± 50	3557–3253	3405
LU-4879	100–110	3290 ± 70	3690–3377	3522
LU-4878	110–120	3200 ± 60	3570–3255	3426
LU-4877	120–130	3300 ± 60	3685–3396	3529

Table 2 (*continued*)

Site name and radiocarbon laboratory code	Core depth (cm)	Radiocarbon date (^{14}C BP)	Calibrated age, 95% range (cal BP)	Calibrated age, Median (cal BP)
LU-4876	130–140	3380 ± 60	3826–3475	3625
LU-4875	140–150	3490 ± 60	3913–3608	3763
LU-4874	150–160	3730 ± 50	4238–3928	4080
LU-4873	160–170	3570 ± 40	3978–3723	3870
LU-4871	180–190	4060 ± 60	4815–4418	4564
LU-4870	190–200	4070 ± 60	4815–4422	4580
LU-4869	200–210	4130 ± 80	4841–4440	4661
LU-4868	210–220	4190 ± 40	4844–4584	4724
LU-4867	220–230	4530 ± 70	5449–4894	5167
LU-4866	230–240	4460 ± 80	5305–4871	5106
LU-4865	240–250	4930 ± 80	5896–5485	5678
LU-4863	260–270	5650 ± 170	6879–6017	6462
LU-4862	270–280	6150 ± 120	7309–6742	7040
LU-4861	280–300	6090 ± 180	7415–6553	6966
LU-4858	310–320	5620 ± 110	6666–6210	6420
LU-4857	320–330	6270 ± 90	7416–6960	7186
LU-4856	330–340	6090 ± 120	7252–6678	6968
LU-4855	340–350	6720 ± 120	7834–7420	7588
LU-4854	350–360	6910 ± 130	7981–7518	7758
Zmeinoe				
LU-5066	20–30	1230 ± 40	1267–1064	1162
LU-5065	40–50	2720 ± 70	2991–2740	2832
LU-5064	60–70	3530 ± 40	3920–3694	3800
LU-5063	80–90	4090 ± 100	4852–4299	4613
LU-5062	100–110	3930 ± 60	4525–4159	4362
LU-5061	120–130	4790 ± 50	5608–5328	5517
LU-5060	140–150	5220 ± 70	6192–5760	5992
LU-5059	160–170	6040 ± 70	7156–6732	6893
LU-5058	180–190	6520 ± 70	7567–7306	7434
LU-5057	200–210	6200 ± 90	7313–6860	7095
LU-5056	220–230	7140 ± 90	8170–7790	7965
LU-5055	240–250	7450 ± 80	8408–8051	8268
LU-5054	260–270	7860 ± 70	8983–8484	8685
LU-5053	280–290	8690 ± 80	10116–9526	9677
LU-5052	300–310	8360 ± 70	9520–9140	9369
LU-5051	320–330	8720 ± 90	10145–9533	9731
LU-5050	340–350	8970 ± 60	10236–9914	10097
LU-5049	350–360	9330 ± 90	10750–10255	10533
LU-5048	360–370	9340 ± 80	10742–10281	10548
LU-5047	370–378	9600 ± 130	11233–10586	10934
LU-5046	378–390	10020 ± 120	11996–11231	11563
LU-5045	390–396	10580 ± 280	13066–11412	12391

birch and alder associations with grasses and sedges occurred in swampy depressions and around the lakes, while steppe-like vegetation with *Artemisia* and Chenopodiaceae likely occupied sunny dry slopes and disturbed soils. Sediment lithology (Table 1) and *Pediastrum* green algae colonies suggest fresh and shallow water sedimentation environments, which became rich in organic matter towards the end of this interval.

LPAZ Ko-6 (715–775 cm) reveals a distinct increase in AP percentages up to 90–95% and absolute dominance of *Pinus* and *Betula* sect. *Albae* pollen, while *Picea* and *Artemisia* are only minor components of the pollen assemblages. The pollen assemblage composition suggests a well-forested landscape with predominance of birch and pine forests. Ferns of the Polypodiaceae family became more abundant in the coastal vegetation at that time.

The LPAZ Ko-5 (585–715 cm) demonstrates stably high AP values (ca. 95%) and prevailing dominance of *Pinus* and *Betula* sect. *Albae* in the pollen assemblage. Cool temperate broadleaf taxa (i.e. *Corylus*, *Ulmus*, and *Tilia*) appear in this zone and show progressively higher values, thus contributing up to 30% to the total pollen sum. The pollen record indicates that further development of the dominant pine and birch forests was accompanied with a gradual spread of cool temperate tree species, suggesting regional climate warming.

LPAZ Ko-4 (335–585 cm) reveals highest contribution of the temperate deciduous tree taxa (i.e. *Corylus*, *Ulmus*, *Tilia*, *Quercus*, and *Fraxinus*) and *Alnus* (up to 40%) to the pollen assemblage. This noticeable increase in the warm-loving taxa percentages is accompanied by relatively low values of *Betula* (15–20%) and *Pinus* (5–15%). *Picea* pollen percentages rise from the middle of this zone and reach up to 17% in the upper part. At the same time, an abrupt increase in Polypodiaceae fern spore percentages (over 40%) and a slight increase in NAP (up to 5%) are registered. Recorded changes in the pollen assemblages suggest that the temperate deciduous broadleaved forests experienced their optimum in the region. Change in the core sediment from gyttja to peat recorded at 440 cm depth (Table 1) indicates a change in hydrological conditions from a shallow lake or pond to a mire. In the diagram (Fig. 3), this change is accompanied by complete disappearance of *Pediastrum* algae colonies and the abrupt increase in Polypodiaceae spores, suggesting a spread of ferns towards the coring site. Increasing *Picea* pollen percentages and decreasing percentages of temperate tree taxa indicate progressive cooling during the second half of this interval.

LPAZ Ko-3 (135–335 cm) reveals substantial decrease in percentages of temperate deciduous taxa and *Alnus*, accompanied by rising values of *Betula*, *Pinus*, and *Picea*. Starting from 210 cm depth, NAP percentages (mainly Cyperaceae and Poaceae) show increase up to 8–12%, which is accompanied by relatively high values of Polypodiaceae fern spores. Pollen spectra suggest that the retreat of

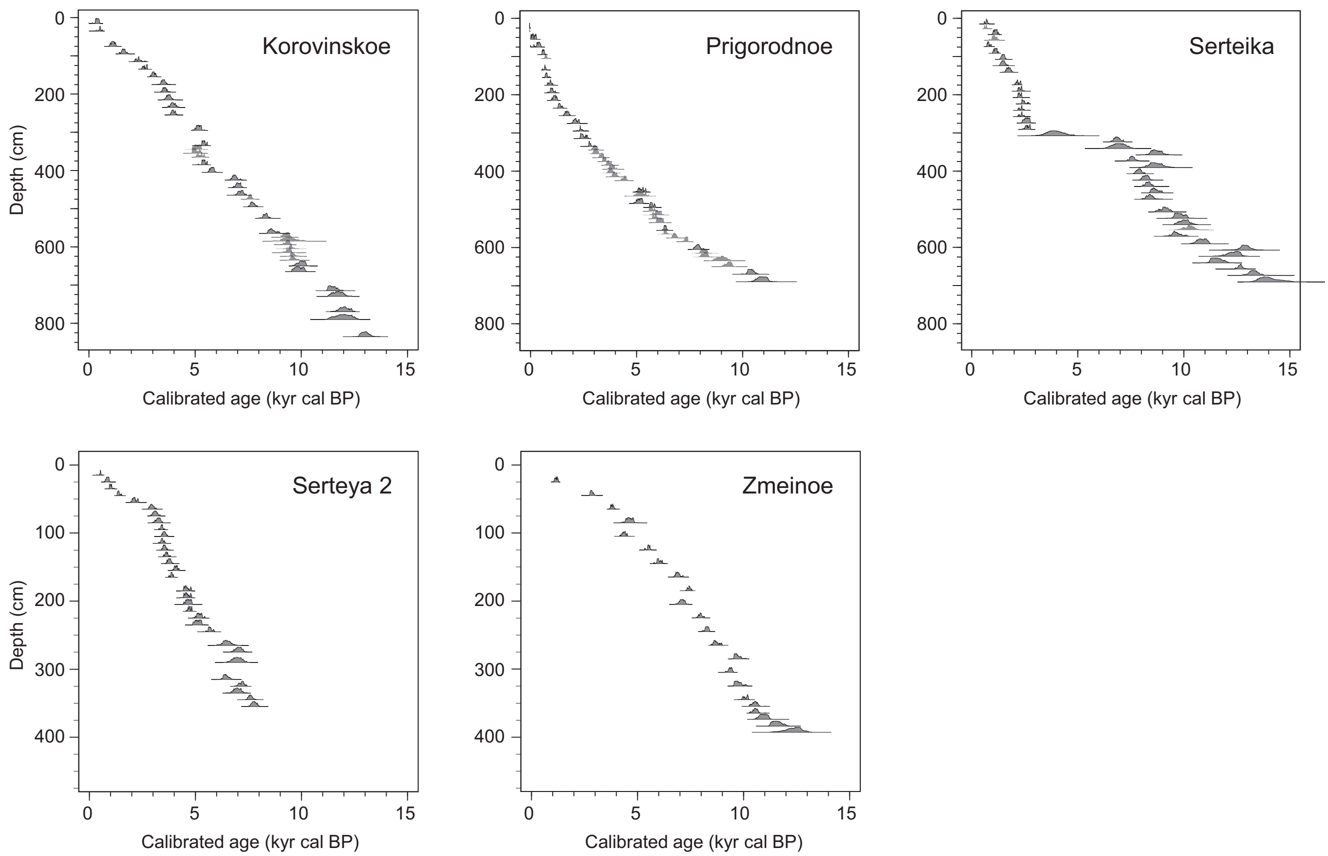

Fig. 2. Calibrated age distribution of the 178 radiocarbon dates (Table 2) obtained for the five sedimentary sequences presented in the current study.

temperate taxa and spread of pine, birch, and spruce forests that started during LPAZ Ko-3 continued in this zone indicating further cooling in the study region. Small peaks in Poaceae and Cyperaceae and the associated decrease in AP pollen percentages registered in this zone may also reflect some opening of the landscape associated with human activities. Findings (although rare) of *Rumex* pollen – one of the most common human indicator taxa (Behre, 2007) – first occur in this zone, supporting such interpretation.

LPAZ Ko-2 (35–135 cm) demonstrates highest percentages of *Picea* pollen (up to 55%) in the lower half of this zone although in the upper half *Pinus* becomes the most important pollen contributor followed by *Picea*, *Alnus*, and *Betula*, while temperate deciduous taxa are only sporadically present. A progressive increase in NAP percentages (from 5 to 25%) is another distinctive feature of this zone. Spread of spruce – a boreal evergreen conifer – reached its culmination in the region at the beginning of this phase, indicating a cool and moist climate. *Sphagnum* mosses start to play a more important role in the vegetation cover. Participation of temperate tree taxa in the forests remains insignificant. Occurrence of *Secale*, *Cerealia*, and *Cannabis*-type pollen in the upper part of this zone associated with a pronounced decrease in AP percentages suggest stronger than before human impact on the vegetation and local cultivation of cereals and hemp.

LPAZ Ko-1 (0–35 cm) also reveals relatively low AP percentages (ca. 50–65%). Major arboreal taxa remain *Pinus*, *Picea*, *Betula*, and *Alnus*. Cyperaceae (sedges) and Poaceae (grasses) are major herbaceous taxa. A number of herbaceous taxa generally regarded as human indicators (i.e. *Cannabis*, *Cerealia*, *Rumex*, and *Secale*) that first time occurred in the upper part of LPAZ Ko-2 remain constantly registered in this zone. The composition of the pollen spectra suggests further decrease of the regional forest cover due to intensified human activities, including animal husbandry and agriculture. Linden, oak, elm, and hazel virtually disappear from the pollen assemblages as the result of unfavorable (cooler) climate but also due to selective use by humans documented in the historical and ethnographic sources.

4.1.2. *Prigorodnoe Mire*

The Prigorodnoe pollen diagram (Fig. 4) is divided into seven major pollen zones.

LPAZ Pr-7 (765–850 cm) reveals a well-defined peak of *Picea* (up to 20%) associated with relatively high pollen percentages of *Pinus* and *Betula* sect. *Albae*. The NAP taxa (mainly *Artemisia*, Cyperaceae, and Poaceae) percentages are minimal in the middle of this zone (15%), but reach up to 40% in the samples from the bottom and the top layers. Sediment lithology and moderately abundant *Pediastrum* green algae point to a fresh and shallow water body relatively poor in organics. The pollen assemblage composition suggests relatively high participation of trees in the vegetation cover and dominance of pine, birch, and spruce in the regional forests.

LPAZ Pr-6 (690–765 cm) differs from the previous zone by relatively high NAP values (up to 50%), a decrease in *Picea* (5–10%) and *Pinus* (10–20%) and a peak in *Artemisia* pollen (up to 23%). High abundances of *Pediastrum* green algae colonies indicate aquatic sedimentation environments. The pollen record suggests opening of the landscape and spread of herbaceous communities with *Artemisia* and Chenopodiaceae occupying drier habitats and those with Poaceae and Cyperceae settling moister habitats.

LPAZ Pr-5 (635–690 cm) reveals a drastic increase in AP (90–95%) and virtual disappearance of *Picea*, *Artemisia*, and

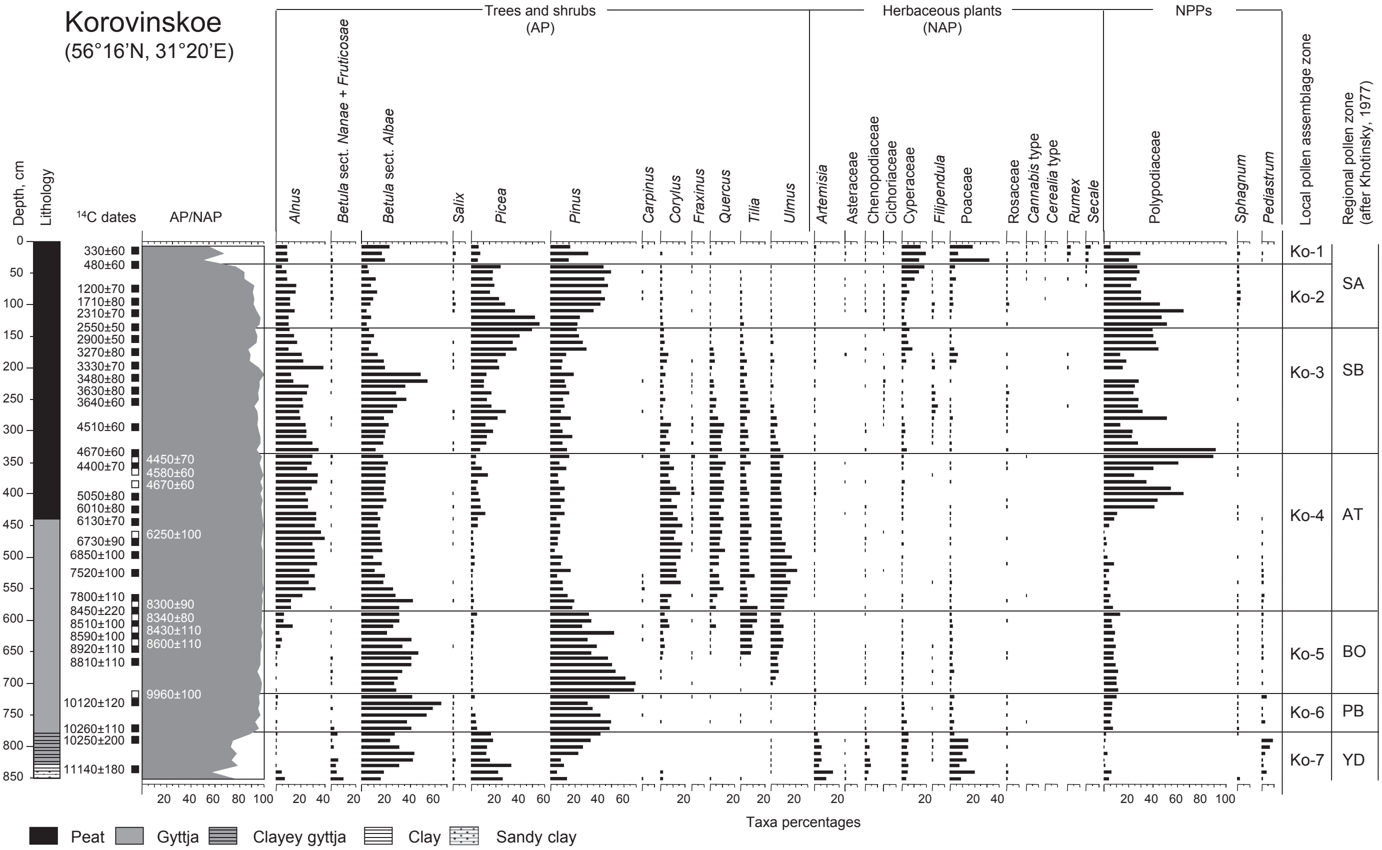

Fig. 3. Pollen percentage diagram and radiocarbon age determinations from Korovinskoe Mire.

Chenopodiaceae from the pollen assemblages. Highest values of *Pinus* (up to 80%) suggest a wide spread of pine forests in the region. Rising percentages of *Ulmus* and *Corylus* indicate presence of elm and hazel in the vegetation and suggest significant warming of the regional climate during this phase. The abundance of organic gyttja (Table 1) also points to a change in sedimentation environments.

LPAZ Pr-4 (445–635 cm) demonstrates highest contribution of *Corylus*, *Ulmus*, *Tilia*, *Quercus*, *Fraxinus*, and *Alnus* to the pollen assemblage suggesting maximum spread of cool mixed and temperate deciduous forests and reduction of birch and pine forests in the region. *Picea* pollen percentages show a rise from the middle of this zone resembling an analog change recorded in the middle of LPAZ Ko-4 of Korovinskoe (Fig. 3). A change in the core lithology from gyttja to peat recorded at 577 cm depth (Table 1) indicates a transition towards the mire phase. In the diagram (Fig. 4), this change is accompanied by a drastic increase in *Sphagnum* spore percentages, suggesting a significant role of peat mosses in the vegetation cover at and around the coring site. Similar to the Korovinskoe record (Fig. 3), increasing *Picea* pollen percentages and decreasing percentages of temperate tree taxa registered in the upper half of this zone can be interpreted as progressive cooling during this interval.

LPAZ Pr-3 (325–445 cm) reveals decrease in percentages of temperate deciduous taxa and *Alnus* accompanied by rising values of *Betula*, *Pinus*, and *Picea*. AP pollen percentages are high suggesting dense forest vegetation around the site.

LPAZ Pr-2 (65–325 cm) shows dominance of *Picea*, *Betula*, and *Pinus* and a minimum pollen contribution from temperate deciduous taxa. AP percentages are still high, though a slight increase in herbaceous pollen (up to 5%) occurs in the upper part of this zone accompanied by rare finds of human indicator taxa pollen.

LPAZ Pr-1 (0–65 cm) reveals a strong reduction in *Picea*, a virtual disappearance of broadleaved temperate deciduous tree taxa, and a noticeable increase in NAP (up to 25%) suggesting moderate deforestation of the landscape and development of secondary birch and pine forests. Intensified human activities such as wood exploitation and agriculture are the main reasons for these changes in the pollen assemblages.

4.1.3. Serteika Mire

The pollen diagram of Serteika (Fig. 5) is divided into six major pollen zones.

LPAZ Sr-6 (750–850 cm) reveals striking similarity to LAPZ Ko-7, in particular, relatively low AP percentages with a co-dominance of *Betula* sect. *Albae* and *Pinus* and *Picea*, relatively high contents of *Betula* sect. *Nanae* + *Fruticosae* and alder, and the highest contents of *Artemisia* and Chenopodiaceae.

LPAZ Sr-5 (650–750 cm) is characterized by a distinct increase in AP percentages and absolute dominance of *Betula* sect. *Albae* and *Pinus* pollen, while *Picea* and *Artemisia* almost disappear from the pollen assemblages.

The LPAZ Sr-4 (550–650 cm) demonstrates stably high AP values (ca. 95%) and further dominance of *Pinus* and *Betula* sect. *Albae*. Cool temperate broadleaf taxa (i.e. *Corylus*, *Ulmus*, and *Tilia*) appear in this zone and show progressively increasing values suggesting significant warming of the regional climate representing the mixed boreal-temperate character of the forest vegetation around the study site.

LPAZ Sr-3 (310–550 cm) reveals highest contents of temperate deciduous tree taxa (i.e. *Corylus*, *Ulmus*, *Tilia*, and *Quercus*) and *Alnus* suggesting spread of temperate deciduous and cool-mixed forests under a significantly warmer than present climate. *Picea*

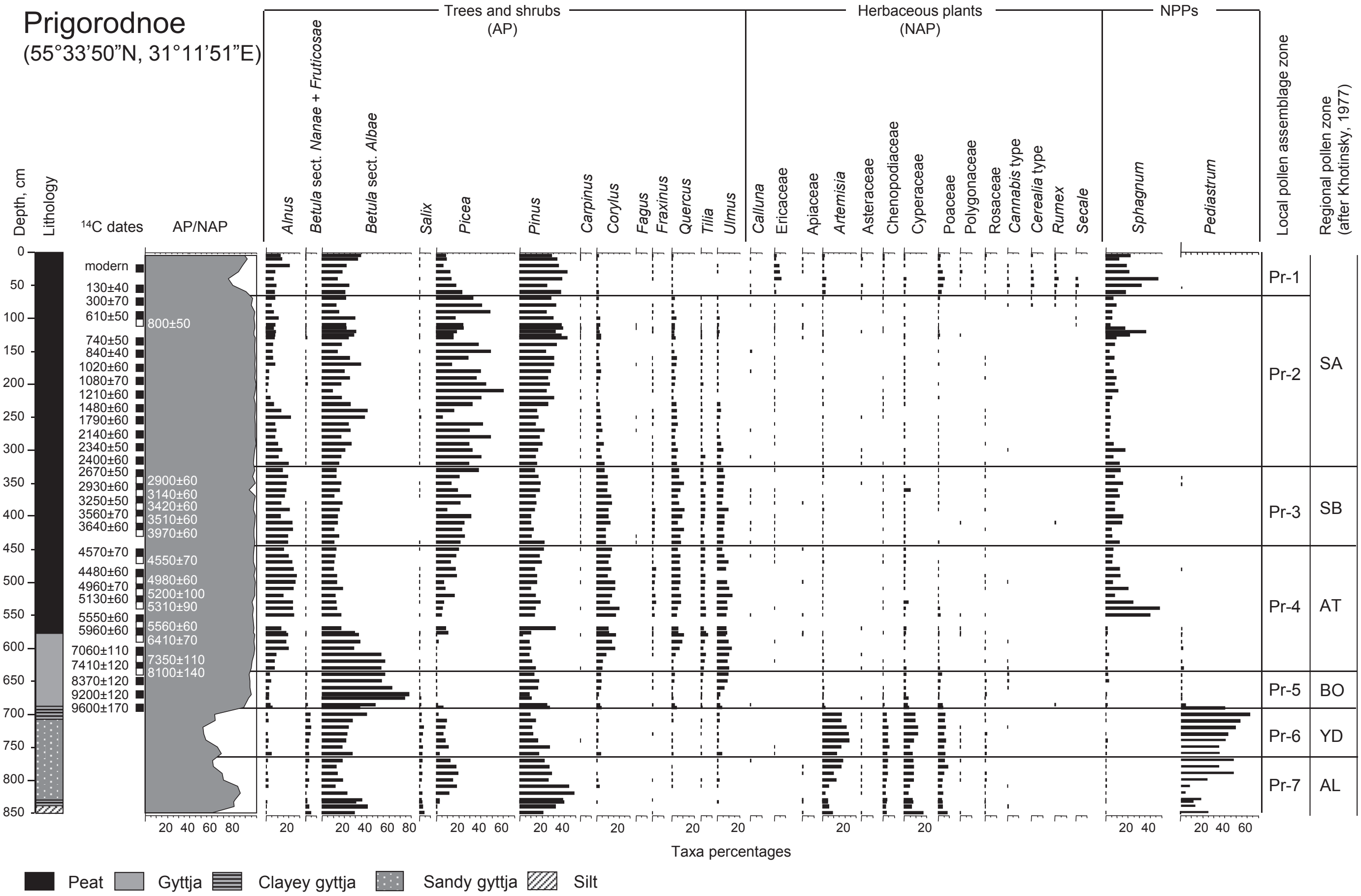

Fig. 4. Pollen percentage diagram and radiocarbon age determinations from Prigorodnoe Mire.

pollen percentages rise from the middle of this zone followed by decreasing percentages of temperate tree taxa reflecting progressive cooling.

LPAZ Sr-2 (60–310 cm) demonstrates highest percentages of *Picea* pollen of the entire Serteika record, though *Pinus*, *Alnus*, and *Betula* remain significant pollen contributors. Very low contents of temperate deciduous taxa coincide with the relatively high NAP contents (20–25%). Occurrence of *Cerealia*-type pollen and increase in Poaceae, Cyperaceae, and Rosaceae in this zone associated with a pronounced decrease in AP percentages suggest stronger than before human impact on the vegetation and local cultivation of cereals.

LPAZ Sr-1 (0–60 cm) reveals further increase in the NAP percentages (up to 30%) accompanied with decreasing percentages of *Picea* and virtual disappearance of *Ulmus* and *Tilia*. Major arboreal taxa remain *Pinus*, *Picea*, *Betula*, and *Alnus*. Cyperaceae, Rosaceae, and Poaceae, including *Cerealia*-type, are major herbaceous pollen taxa.

4.1.4. Serteya 2 Mire

The Serteya 2 pollen diagram (Fig. 6) is divided into five major pollen zones.

LPAZ Se-5 (425–465 cm) reveals relatively high AP values (85–90%) mainly represented by *Pinus* and *Betula* sect. *Albae*. Pollen of *Picea* and *Alnus* are virtually absent, while *Ulmus* and *Tilia* are rather representative temperate deciduous taxa. *Artemisia* pollen grains are rare and Chenopodiaceae is not registered in the pollen assemblages.

LPAZ Se-4 (225–425 cm) demonstrates highest contribution of *Corylus*, *Ulmus*, *Tilia*, and *Quercus* to the pollen assemblage suggesting maximum spread of cool mixed and temperate deciduous forests and reduction of birch and pine forests around the study site. *Picea* pollen percentages show increase from the middle of this zone. Pollen grains of *Trapa natans* (water chestnut) are registered through this pollen zone and its nuts are reported from the 242 cm depth (Table 1). The organic gyttja sediment (Table 1) and relatively high values of *Pediastrum* (Fig. 6) suggest swampy sedimentation and (at least partially) relatively high water level at the coring site.

LPAZ Se-3 (65–225 cm) reveals decrease in percentages of temperate deciduous taxa accompanied by high values of *Betula*, *Pinus*, *Picea*, and *Alnus*. AP pollen percentages are high, though slightly lower than in the previous zone, suggesting some opening of the forest around the coring site.

LPAZ Se-2 (35–65 cm) shows dominance of *Picea* and *Pinus* and minimal pollen contribution of temperate deciduous taxa. A progressive decrease in AP percentages from 90 to 75% occurs in this zone accompanied by an increase in Cyperaceae.

LPAZ Se-1 (0–35 cm) reveals a strong reduction in *Picea* and *Pinus* percentages, but a relative increase in *Alnus* and *Betula* sect. *Albae*. A maximum increase in NAP (up to 30%) in the middle of this zone is accompanied by the appearance of *Cannabis*, *Secale*, and *Cerealia*-type pollen grains suggesting moderate deforestation of the landscape, development of secondary birch forests, and intensified human activities. The topmost two samples of this zone demonstrate a relative increase in AP (up to 85–90%) associated with an increase in *Picea* and temperate deciduous taxa (i.e.

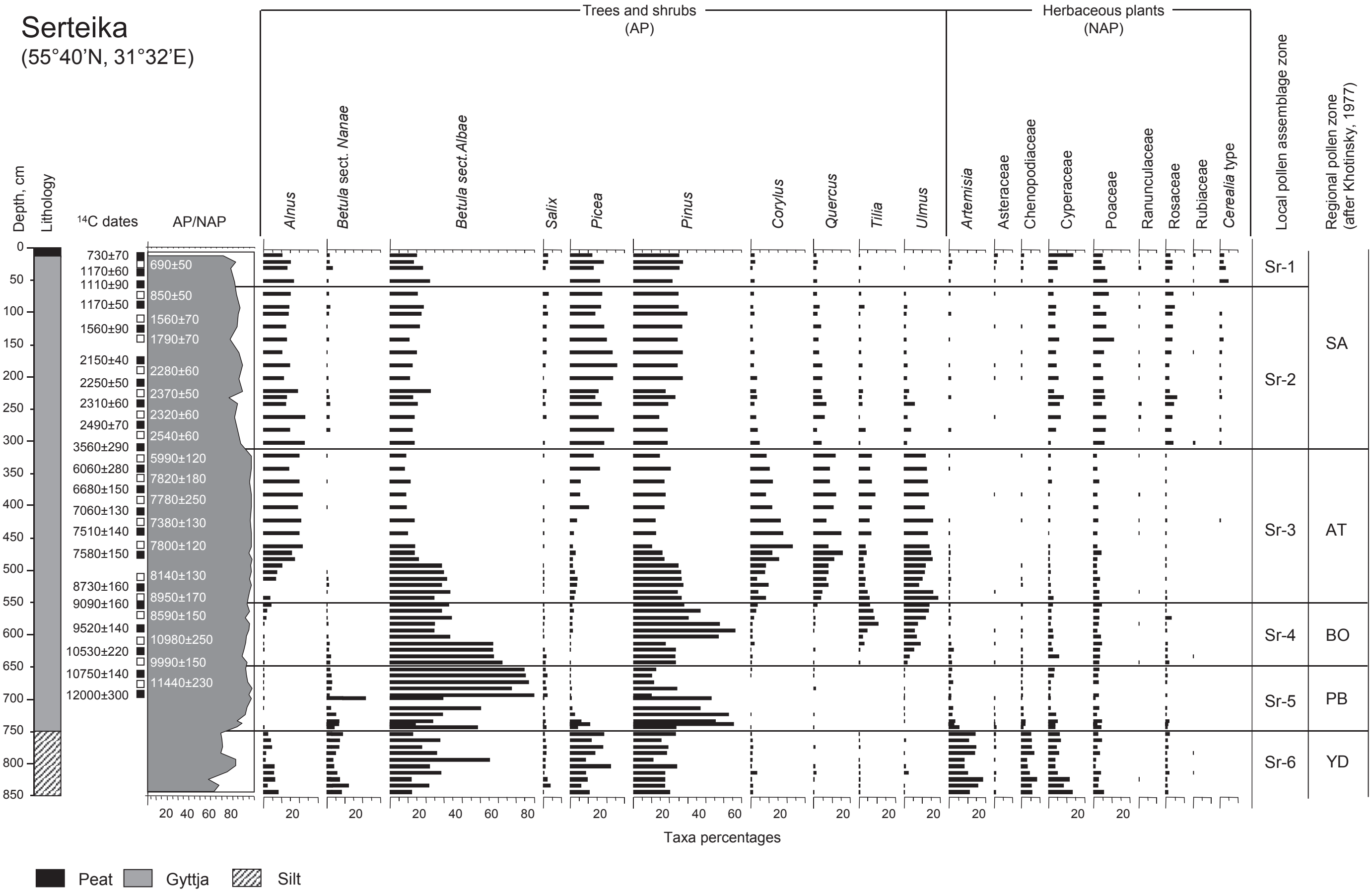

Fig. 5. Pollen percentage diagram and radiocarbon age determinations from Serteika Mire.

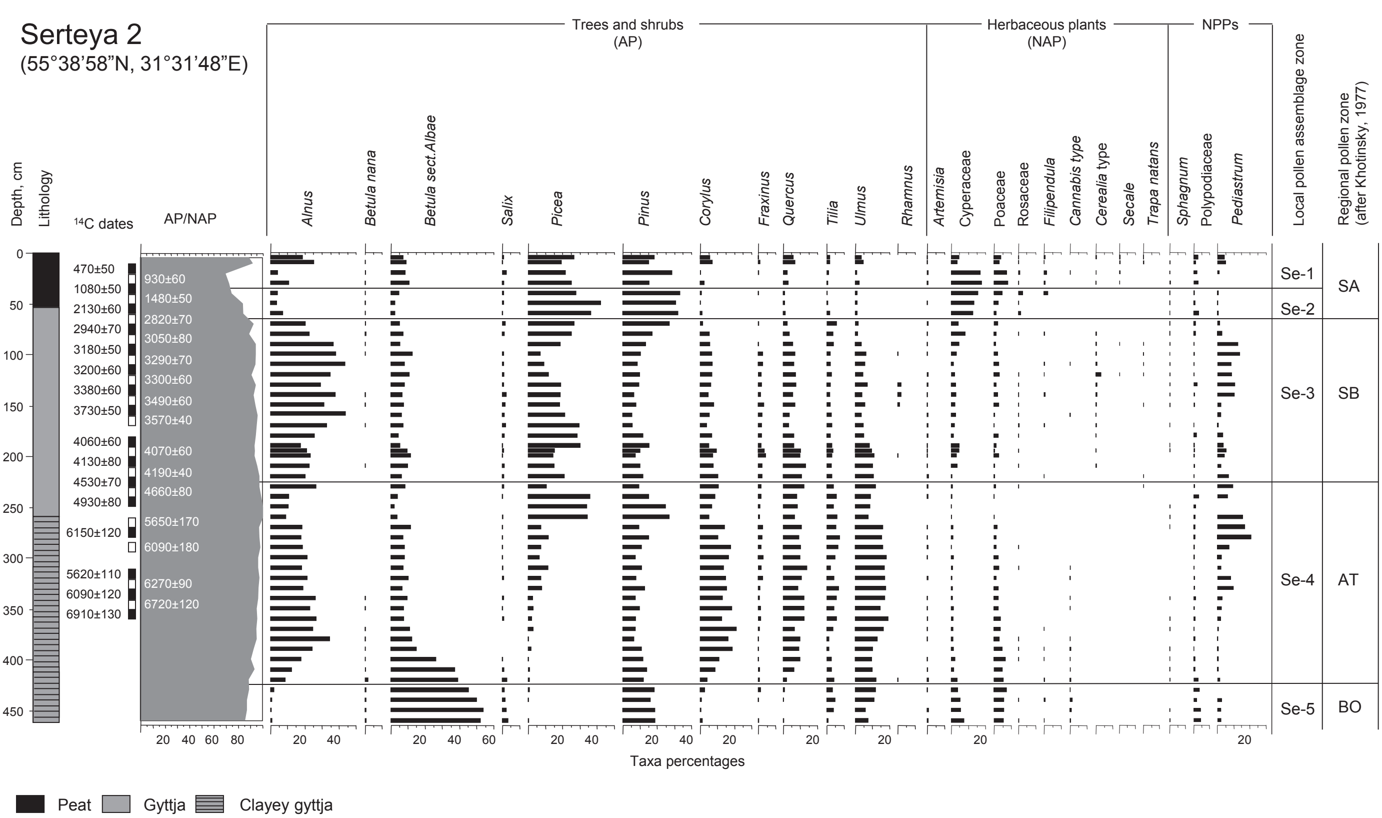

Fig. 6. Pollen percentage diagram and radiocarbon age determinations from Serteya 2 Mire.

Quercus, *Ulmus*, and *Tilia*) percentages. These changes together with extremely rare human indicator taxa pollen may indicate less intensive human activities in the area close to the site and partial recovery of the natural forest vegetation.

4.1.5. Zmeinoe Mire

The pollen diagram of Zmeinoe (Fig. 7) is divided into eight major pollen zones.

LPAZ Zm-8 (432–450 cm) reveals a well-defined peak of *Picea* (up to 40%) accompanied by relatively high pollen percentages of *Pinus* and *Betula* sect. *Albae*. The NAP taxa (mainly *Artemisia*, Chenopodiaceae, Cyperaceae, and Poaceae) percentages are minimal (10–20%) in the middle of this zone.

LPAZ Zm-7 (395–432 cm) demonstrates relatively high NAP values (up to 50%), decrease in *Picea* and *Pinus*, and peaks in shrubby birch, *Artemisia*, and Chenopodiaceae pollen percentages suggesting reduction of the woody cover and opening of the landscape under a cold and relatively dry climate.

LPAZ Pr-6 (365–395 cm) reveals a drastic increase in AP (up to 90%) and virtual disappearance of *Picea*, *Artemisia*, and Chenopodiaceae from the pollen assemblages. Highest values of *Betula* sect. *Albae* and *Pinus* suggest wide spread of birch and pine forests in the region.

LPAZ Pr-5 (275–365 cm) shows further increase in AP (up to 95%). *Pinus* and *Betula* sect. *Albae* remain major pollen taxa, however, cool-temperate deciduous taxa appear in this zone and *Ulmus* pollen percentages become moderately abundant by the end of this phase.

LPAZ Pr-4 (95–275 cm) demonstrates the highest contribution of *Corylus*, *Ulmus*, *Tilia*, *Quercus*, *Fraxinus*, and *Alnus* to the pollen assemblage and a reduction in *Betula* and *Pinus* percentages. *Picea* percentages show a rise from the middle of this zone. A similar (though more pronounced) increase has been noted in the other records (Figs. 3-5).

LPAZ Pr-3 (45–95 cm) reveals a decrease in percentages of temperate deciduous taxa and *Alnus* accompanied by rising values of *Pinus* and *Picea*. *Sphagnum* spores are abundant suggesting well-developed moss covering the peat surface. AP pollen percentages are high suggesting dense forest around the site.

LPAZ Pr-2 (25–45 cm) shows a dominance of *Betula* and *Pinus*, substantially lower percentages of *Picea*, and minimal contribution of temperate deciduous taxa pollen. AP percentages are still high, though an increase in NAP (up to 15%) occurs in the upper part of this zone accompanied by finds of human indicator taxa pollen, including cereals.

LPAZ Pr-1 (0–25 cm) reveals a strong reduction in *Picea*, virtual disappearance of broadleaved temperate deciduous tree taxa, and a noticeable increase in NAP (up to 30%) suggesting moderate deforestation of the landscape and development of secondary birch and pine forests. Intensified human activities are suggested by changes in the pollen assemblages. The relative increase in Ericaceae pollen (up to 10%) likely indicates a spread of heath family plants following the deforestation. Pollen grains of *Secale* and *Cerealia*-type are proofs for agriculture.

4.2. Pollen-based correlation: site-specific features and regional trends

Reconstructing the Lateglacial–Holocene vegetation dynamics in the study region and checking the synchronicity of vegetation changes across CER are among the aims of this study. Comparison of the pollen diagrams (Figs. 3-6) and the site-by-site interpretations of the pollen assemblages presented in sections 4.1.1–4.1.5 demonstrates great similarities of the local pollen/

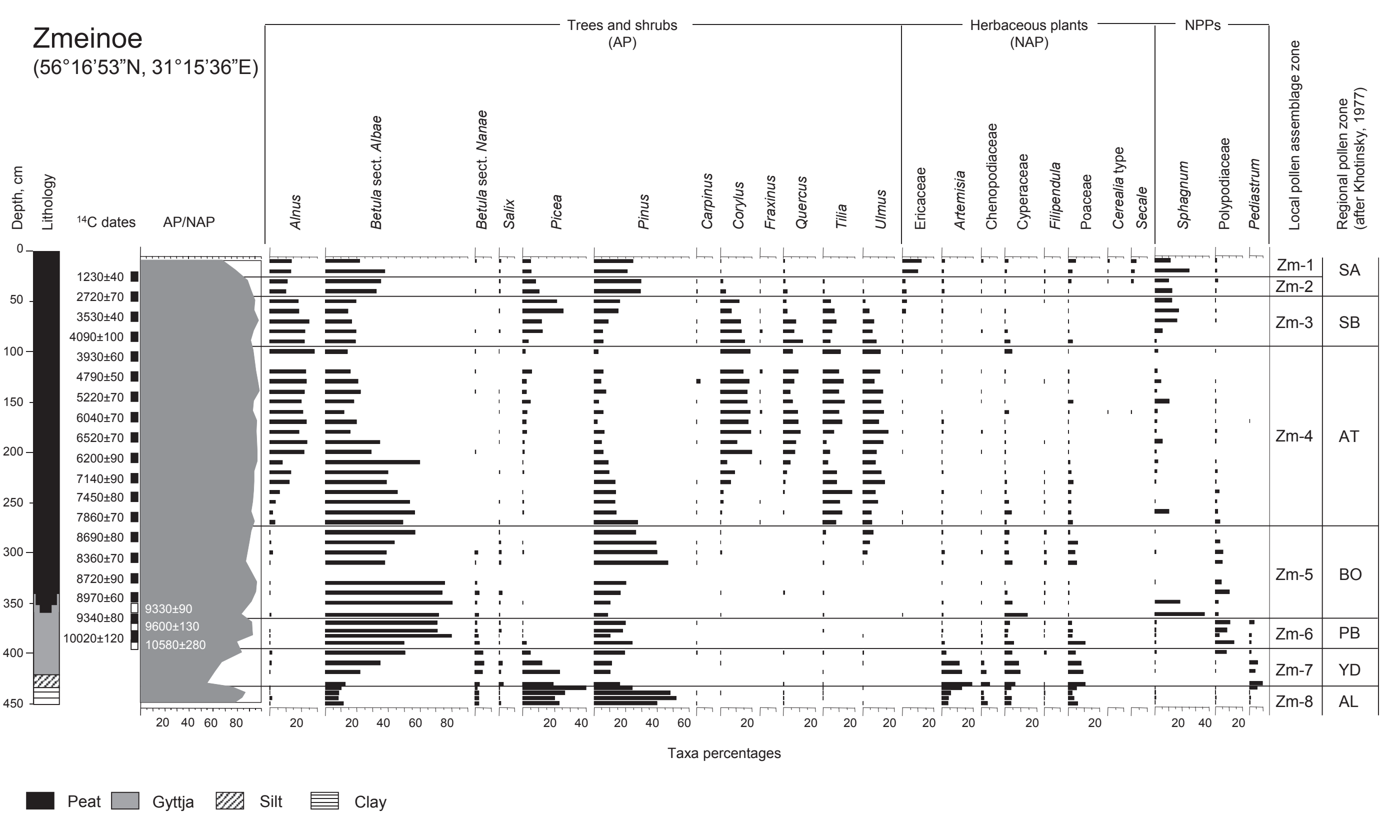

Fig. 7. Pollen percentage diagram and radiocarbon age determinations from Zmeinoe Mire.

vegetation successions with the regional pollen chronostratigraphy and vegetation development scheme suggested for the entire region (Fig. 8; Khotinsky, 1977, 1980). The observed variability in the individual taxa percentages between the five analyzed records can be explained by local differences in microclimatic and environmental conditions between the sites.

The results summarized in Fig. 8 demonstrate straightforward biostratigraphical correlation with the regional Holocene stratigraphy and allow assignment of the identified LPAZ 5 through 1 of the Korovinskoe and Zmeinoe records to the Preboreal, Boreal, Atlantic, Subboreal, and Subatlantic, respectively. The Prigorodnoe and Serteya 2 records do not have pollen assemblages/sediments, which can be attributed to the Preboreal, and the Serteika record likely experienced a hiatus (or extremely low sedimentation rates) during the Subboreal period of the Holocene interval.

The lowermost LPAZ Ko-7 in Korovinskoe, LPAZ Pr-6 and Pr-7 in Prigorodnoe, LPAZ Sr-6 in Serteika as well as LPAZ Zm-7 and Zm-8 in Zmeinoe can be undoubtedly attributed to the Lateglacial interval in the CER region based on the relatively low AP percentages and relatively high percentages of *Picea* and *Artemisia* (Fig. 8; Khotinsky and Klimanov, 1997; Velichko et al., 1997). It is plausible that the oscillation in the AP percentage curve in the bottom part of the Prigorodnoe and Zmeinoe records may represent the Yonger Dryas and the Allerød (Fig. 8), although this assumption cannot be approved by the available radiocarbon dates (Table 2). However, the relatively high percentages of AP and *Picea* and relatively low proportions of *Artemisia* pollen in our records do not support a treeless tundra-steppe landscape, which has been initially suggested for the Younger Dryas (Khotinsky, 1977). The later interpretation of the pollen diagram from the Polovetsko-Kupanskoe record reconsiders the initial interpretation (i.e. Khotinsky, 1977) concluding that a comparatively high content of spruce pollen during the Younger Dryas interval is indicative of continuous occurrence of spruce forests under conditions of partly degrading permafrost (Khotinsky and Klimanov, 1997). A single bulk radiocarbon date (11,140 ± 180 ^{14}C BP) from the 830–840 cm depth in Korovinskoe (Fig. 4) converted into calendar years falls within the 12,700–13,320 cal BP interval (95% range; Table 2) suggesting deposition during the Allerød–Younger Dryas transition or even during the final stages of the Allerød interval. The date (10,250 ± 200 ^{14}C BP) from the 780–800 cm interval falls within the relatively broad interval 11,290–12,560 cal BP, which may represent the Younger Dryas or the early Holocene. More precise age determination is hardly possible without AMS dates on terrestrial plant macrofossils (e.g. Heikkilä and Seppä, 2010; Veski et al., 2012). Such dates are still extremely rare in the entire CER region (Wohlfarth et al., 2007). Wohlfarth et al. (2006) studied sediments of Lake Nero (57°10′25″N, 39°25′36″E) and two other lakes from

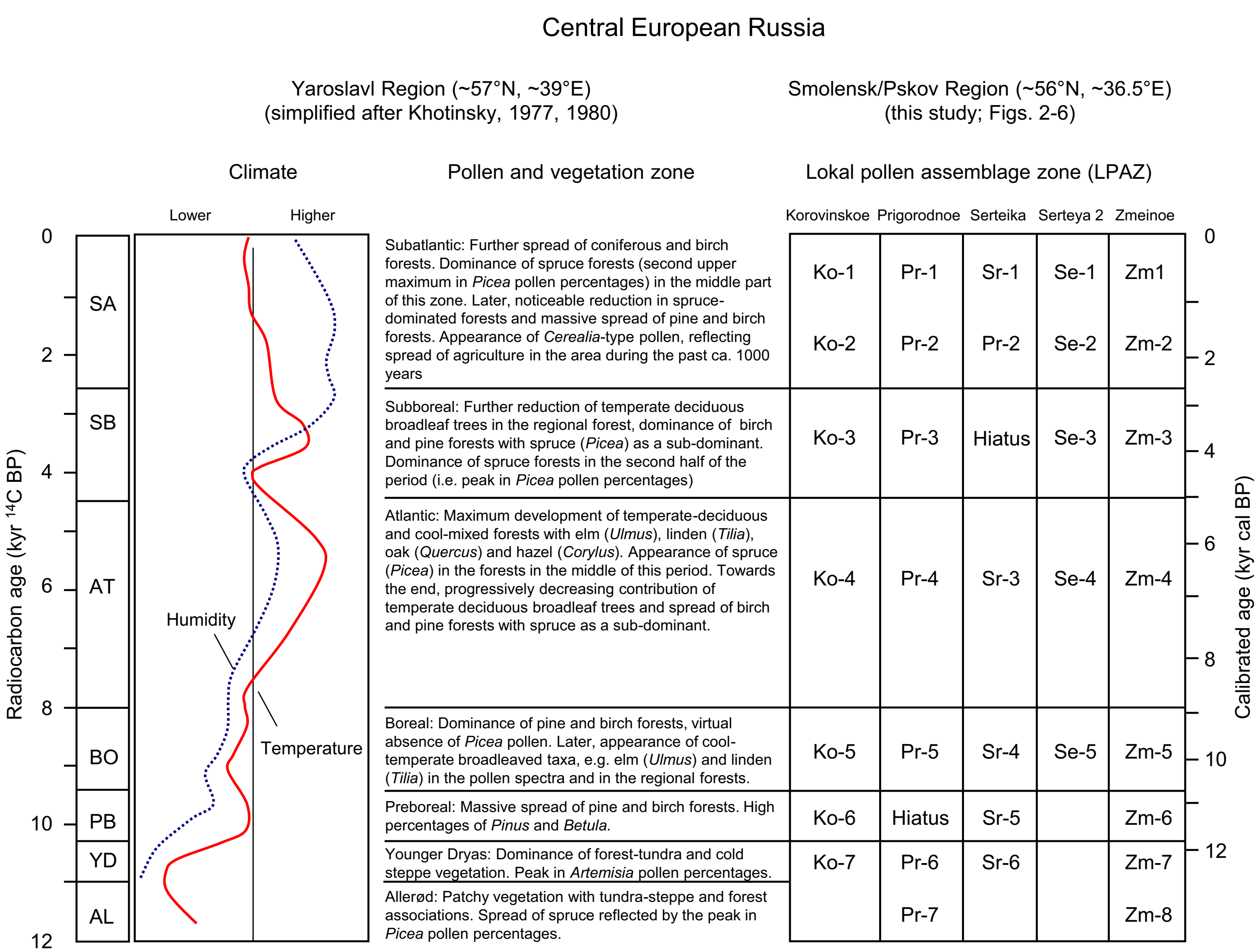

Fig. 8. Local pollen assemblage zones identified in the five pollen records analyzed in the current study (right) correlated to the regional pollen-based climate and vegetation stratigraphy suggested for the Central European Russian region (after Khotinsky, 1977, 1980).

the Yaroslavl region north of Moscow (Fig. 1) to gain information on palaeoclimatic and palaeoenvironmental changes during the past 15,000 years. Their multi-proxy study included pollen, macrofossils, mineral magnetic measurements, and total carbon, nitrogen, and sulphur analyses chronologically constrained by AMS ^{14}C measurements on bark, wood, and leaf fragments. Increased lake productivity and higher mean summer temperatures are reconstructed after 14,500 cal BP. Pollen and plant macrofossil records (Wohlfarth et al., 2006) suggest that *Betula* sect. *Albae* and *Picea* became established close to the site as early as 14,000 cal BP; though the Lateglacial vegetation around the lake was still dominated by *Betula* and *Salix* shrubs and various herbs (NAP up to 45–70%). However, major hydrological changes in the region led to distinctly lower lake levels and caused a sedimentary hiatus in Lake Nero between ca. 13,000 and 8200 cal BP (Wohlfarth et al., 2006) preventing from direct comparison of the Younger Dryas and Preboreal zones in the Nero record with the contemporaneous pollen data presented in the current paper. The bulk radiocarbon dates from the layers in Polovetsko-Kupanskoe assigned to the Younger Dryas suggest significantly older ages (Khotinsky, 1977; Khotinsky and Klimanov, 1997). This supports the common opinion that bulk radiocarbon dates obtained on organic-poor Lateglacial limnic sediments may differ from those obtained from AMS-dated terrestrial material being up to 2000 years older (Litt and Stebich, 1999).

These days, the AMS technique becomes more prevalent in radiocarbon dating. However, neither conventionally obtained radiocarbon dates are out of use (e.g. Chairkina et al., 2017), nor AMS-based chronologies are free from errors and absolutely reliable. Moreover, it is difficult to say that the scientific community has come to the conclusion that conventional dates tend to produce systematically older (i.e. inaccurate) dates than AMS dates. In fact, large-scale inter-laboratory comparisons (e.g. Boaretto et al., 2002) seem to have confirmed that there are no significant differences between results from these two methods, although in general less amount of sample material is needed for the AMS technique. Given the large number of dated organic mud or peat samples from the Holocene sediment available in this study (Fig. 2; Table 2), the use of conventional technique is well justified in the first place.

The AMS dated Lake Nero record suggests that mixed broad-leaved and coniferous forests were widespread in the Yaroslavl region between 8200 and 6100 cal BP and dense, species-rich forests dominated the landscape prior to ca. 3000 cal BP. This entire interval was likely the warmest of the studied sequence (Wohlfarth et al., 2006) and is in line with the regional pollen records from the earlier publications and the current study (Fig. 8; Khotinsky, 1977; Khotinsky and Klimanov, 1997). The high-resolution records from Lake Nero indicate another sedimentary hiatus prior to ca. 2500 cal BP (Wohlfarth et al., 2006), which could be correlated with the hiatus (or extremely slow sedimentation) revealed by the radiocarbon and pollen data from Serteika (Fig. 5) during the Subboreal period (Fig. 8).

At the beginning of the Subatlantic interval, i.e. about 2500 cal BP, pollen percentages for *Pinus*, *Alnus*, *Betula* sect. *Albae*, and particularly for *Picea* increase and pollen percentages for *Tilia*, *Quercus*, *Ulmus*, and *Corylus* decrease distinctly in the pollen diagrams from the Yaroslavl region (Fig. 8; Khotinsky and Klimanov, 1997; Wohlfarth et al., 2006) in line with the regional pollen records from the Smolensk and Pskov regions (Figs. 3–7) presented here.

4.3. Chronological issues

The age determinations obtained through radiocarbon dating of bulk organic samples (Table 2) and pollen-based correlation with the regional biostratigraphy (Fig. 8) suggest that among the analyzed sequences the Korovinskoe Mire contains the most complete sedimentary archive of the Holocene with relatively constant sedimentation rates (ca. 15 yr/cm) and no major reversals or hiatuses. The Bayesian approach was applied to the Korovinskoe dataset in order to build a robust age-depth model (Fig. 9) for this representative pollen record, which is used for inter-regional comparison in the following Discussion chapter.

5. Discussion

5.1. Traces of human impact and agriculture

The five pollen records presented in the current study reveal some changes, which can be interpreted in terms of growing human impact on the natural forest vegetation and agricultural land use. The AP percentages from Korovinskoe show increase through the lower part of the record up to 500 cm depth. The slight decrease in AP percentages is registered at 485 cm depth (Fig. 3) suggesting an initial opening of the pristine forest around the site. The fact that it is not accompanied by any distinct change in the pollen composition may point to men as the driving force for this change. The calibrated radiocarbon dates from the 495 and 475 cm levels allow dating this event to about 7700–7600 cal BP (Table 2). Since then, the pollen spectra demonstrate a more or less continuous decrease in AP content suggesting increasing opening of the surrounding landscape, likely associated with human activities. An abrupt increase in Polypodiaceae fern spores registered from 425 cm depth (Fig. 3) is another strong evidence for opening of the forest canopy, which occurred since about 7100–7000 cal BP. The second shift in AP percentages towards distinctly lower values occurred at 200 cm depth (Fig. 3), i.e. after 3750 cal BP, and the third even more dramatic decrease started from 70 cm depth, i.e. since about 1000 cal BP (Table 2). First appearance of single *Rumex* (sorrel) pollen grains starts from ca. 4200 cal BP, followed by the appearance of cultivars such as *Cerealia*-type pollen since ca. 1400 cal BP and *Secale* (rye) pollen during the last millennium. This pattern of changes may indicate changing human activities and land use close to the site since the Neolithic starting from the use of wood for construction and making fire by the local sparse hunter-

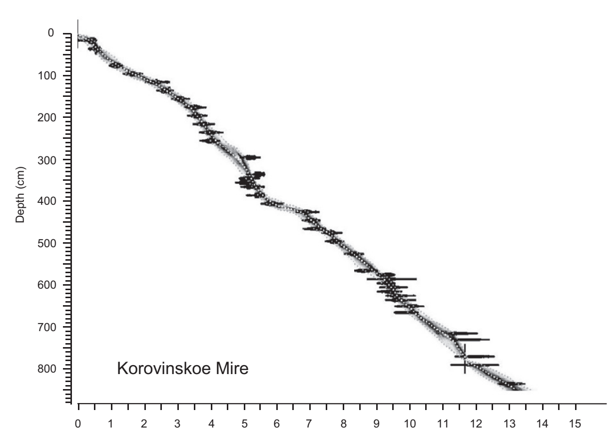

Fig. 9. Bayesian age-depth model constructed for the Korovinskoe core plotted along with the unmodeled calibrated age distributions of the radiocarbon dates (see Table 2 for details). The white dotted line represents modeled calibrated median values. The two grey dotted lines indicate the 95% probability range of the age model. Within the 95% probability range, darker shadows indicate higher modeled probability density and lighter shadows indicate lower probability density.

fisher-gatherer population and culminating in the shift to agriculture.

In contrast to the rather synchronous patterns of natural vegetation development (Fig. 8), changes, which could be assigned to human activities, demonstrate substantial temporal variability. Thus, the Prigorodnoe pollen diagram (Fig. 4) reveals stable, very high AP values during the entire middle Holocene suggesting undisturbed local forest at and around the site. A small decrease in AP (and increase in Cyperaceae percentages) registered in a single sample at 360 cm (ca. 3300–3200 cal BP) may indicate a short-term intervention of prehistoric men, but could be also explained by a number of other non-anthropogenic factors. The first appearance of human indicator pollen (i.e. *Secale*) accompanied by a slightly decreasing trend in the AP curve of the Prigorodnoe record is dated to 700–600 cal BP. However, the major drop in AP percentages and the appearance of several human indicator pollen taxa indicating forest clearance and intensified agriculture can be traced only during the last 500 years.

The Serteika (Fig. 5) and Serteya 2 (Fig. 6) records are located close to each other (Fig. 1) at a distance of ca. 1.5 km in the valley of the Serteya (also named Serteika) River – a small left tributary of the Western Dvina. In the pollen record from Serteya 2 the initial decrease in AP percentages coincides with the first appearance of *Trapa natans* and is dated to ca. 5200–5100 cal BP. A weak decrease in AP continues during the next 3000 years and is followed by a more steady drop in AP (and associated increase in Poaceae and Cyperaceae percentages) between ca. 3200/3000 and 500 cal BP. Pollen grains of *Cerealia*-type and *Secale* are discontinuously present in the record during the last 5000 years, however, in extremely low quantities. In the Serteika pollen diagram (Fig. 5) the initial decrease in the AP percentages cannot be securely dated because of a sedimentary hiatus, which occurred sometime between ca. 6800 and 2600 cal BP. A continuous decrease in AP percentages is registered between ca. 2600 and the youngest layers (i.e. 700–600 cal BP) of this sedimentary section. *Cerealia*-type pollen grains are continuously traced during this time interval becoming more abundant after ca. 1200/1000 cal BP.

In the pollen record of Zmeinoe (Fig. 7) single pollen grains of *Secale* and *Cerealia*-type appear for the first time in the diagram about ca. 6700 cal BP, though not recorded during the following ca. 5500 years (i.e. until ca. 1200 cal BP). The Holocene trend towards lower AP values only starts at 140 cm, i.e. after 6000 cal BP. The slight decrease in AP percentages changes to a steadier drop after ca. 3800 cal BP and then by ca. 1200 cal BP.

The pollen records discussed in the current study suggest intensification of human activities in the region during the past 7000 years, particularly visible by decreasing percentages of trees and shrubs. Though, the pollen data does not show a synchronous pattern of changes during the early period (i.e. prior to 4000 cal BP), which can be easily explained by a low density and uneven distribution of prehistoric hunter-fisher-gatherer population in this densely forested region. However, stepwise strengthening of human impact on the initially dense forest vegetation can be suggested after ca. 4200/3700 and particularly during the last 1400/1000 years.

The pollen diagram of Polovetsko-Kupanskoe in the Yaroslavl region (Khotinsky, 1977; Khotinsky and Klimanov, 1997) does not show a relationship between AP and NAP and, therefore, does not allow a direct comparison with the pollen records presented here. However, traces of *Cerealia*-type pollen in Polovetsko-Kupanskoe do not occur prior to 1150 ± 70 ^{14}C BP (i.e. ca. 1200 cal BP) and the peak of cereals (and other human indicator taxa) in the pollen diagram has been dated to ca. 400/500 cal BP (Khotinsky and Klimanov, 1997). The uppermost pollen zone in the Lake Nero diagram (Wohlfarth et al., 2006) is characterized by a decrease in pollen percentages and concentrations for trees and an increase in Poaceae pollen percentages and concentrations. Pollen of *Secale cereale* (rye), *Rumex acetosa/acetosella* (sorrel), *Urtica* (nettles), *Fagopyrum* (buckwheat), and *Linum* (flax) demonstrate agricultural activity close to the site over the last 500 years. However, since the settlement of Rostov at Lake Nero has been reported in the Russian chronicles since 862 AD and became a very important Russian city by the 10th century, the absence of taxa indicating agricultural activity during ca. 1200–500 cal BP (as in Polovetsko-Kupanskoe) was assigned to a sedimentary hiatus in the analyzed core (Wohlfarth et al., 2006).

The Holocene pollen record Staroselsky Moch (Fig. 1) from a large mire situated at the watershed between the Western Dvina and Volga rivers in the southern part of the Valday Upland also demonstrates stably high AP percentages through the entire middle Holocene, i.e. between 5700 and 1700/1800 cal BP and a progressive increase in NAP and human indicator taxa, including *Cerealia*-type pollen between 1700/1800 and 400/500 cal BP (Novenko et al., 2009; Novenko and Olchev, 2015). The occurrence of single pollen grains of *Cerealia*-type is registered at ca. 3400 cal BP preceded by the minor (one sample) oscillation in the AP values and appearance of Onagraceae (e.g. *Chamerion angustifolium*) pollen (Novenko et al., 2009) suggesting a short-term opening of the forest, possibly with the help of fire, and occurrence of a small-scale field or garden close to the study site.

Thus, the pollen records from the cool-mixed forest zone of CER suggest a long period of human presence with a relatively minor impact on the forest vegetation during the middle Holocene phase. Human impact becomes more visible in the diagrams during the past three to four thousand years but did not left distinctive traces (exceeding the natural Holocene AP/NAP variations) in the pollen records prior to 3000/2500 cal BP or even later. These results support the hypothesis that the vegetation cover of CER was under natural control during most of the Holocene and that the pollen records from this region can therefore serve as reliable climate archives, whose potentials, however, remain underexploited until today. Our data corroborate recent results of pollen and charcoal analyses from subtropical China (Ma et al., 2016; Zhao et al., 2017) suggesting that this initially densely forested area experienced primary hunter-fisher-gatherer occupation during a much longer period than traditionally believed and was not markedly affected by agricultural activities until ca. 3000 cal BP.

Archaeological research in the region of Smolensk has a long history going back to the second half of the XIX century. During recent decades more attention was paid to the Mesolithic and Neolithic habitation in the Western Dvina and Lovat river basins (e.g. Miklyaev, 1995; Dolukhanov et al., 2005, 2009; Mazurkevich et al., 2009). The investigations started in 1972 by the discovery of a submerged dwelling site of Neolithic age in the Serteika River valley (Miklyaev, 1995). The following archaeological surveys conducted by Russian and international teams led to the discovery of over 40 new sites there (Mazurkevich et al., 2009) and allowed to reconstruct the occupation history of the Serteika valley by prehistoric hunter-fisher-gatherers since about 8500 years ago (Mazurkevich et al., 2009). The sites attributed to the earliest occupation phase are considered campsites; they included remains of circular dwelling structures with post-holes and circular fireplaces and diverse stone artifacts. The cultural layer with the earliest pottery remains has been dated to ca. 8175 ± 300 cal BP based on wood fragments. The number of sites and artifacts increases during the following period between 8000 and 6500 cal BP, while the faunal and plant macrofossil remains obtained from these cultural layers suggest that these early pottery-making communities subsisted on wildlife resources obtained by hunting, fishing, and gathering (Mazurkevich et al., 2009). Numerous pile dwelling structures excavated in the Serteya valley and at lakes Usvyaty (55°43′N, 30°47′E) and Zhizhitskoe (56°14′N, 31°15′E) in the neighboring Pskov region were securely dated to the interval ranging from ca. 6400 to ca. 4000 cal BP. The plant and animal remains from the pile dwelling sites also suggest high reliance on wild resources. Mazurkevich et al. (2009) report 40 animal species, which were hunted for meat and fur (e.g. elk, brown bear, wild boar, marten, otter, squirrel, etc.), along with numerous fish bones and seeds of at least 30 edible wild plants, including hazelnut and water chestnut. Spruce, pine, ash, maple, and seldom oak trees were used as construction material. A limited number of domesticates (cattle, sheep/goat, and pig) only appear in the bone assemblages from the cultural layer dated to 4150–3830 cal BP (Mazurkevich et al., 2009).

Referring to the results of pollen analysis from the archaeological site Serteya 2 and from the Naumovo site at Lake Zhizhitskoe in the Pskov region, Mazurkevich et al. (2009) suggest an initial onset of small-scale agriculture during the pile dwelling phase of the Usvyatian Culture (ca. 6600–5400 years ago) and established slash-and-burn (swidden) agriculture during the Zhizhitsian Culture phase, ca. 4300–4200 years ago. If true, such very early onset of agriculture in the study region deserves serious attention requiring a more careful investigation and discussion (Königsson and Possnert, 1997).

While some earlier studies place the onset of slash-and-burn agriculture in the boreal forest zone of CER to as early as the second millennium BC, others argue that this practice did not play any important role until the VIII/IX century AD. Summarizing all *pros* and *contras*, Slobodin (1952) suggested that during the whole second and most of the first millennium BC prehistoric cultures in the forest zone of CER practiced a small-scale ('gardening') agriculture that played a minor role in the subsistence mainly based on hunting and fishing. Following recent concepts of subsistence economy (Smith, 2001), these cultures may be characterized as 'complex hunter-gatherers' with a mixed subsistence based on both foraging and a low-level food production. The importance of agriculture in the CER region steadily grew with the appearance of hill fort settlements (*gorodishche*) during the Iron Age, and carbonized grains of barley, wheat, millet, and pea were reported from the sites near Smolensk and in the northern part of Belarus dating to the VI–XI centuries AD (Slobodin, 1952).

Recent data from the broader Baltic Sea region are important for discussing dispersal routes and a possible early onset of agriculture in the CER region. The earliest directly dated barley grain from Bornholm Island in the western Baltic Sea is ca. 5780 year old and the Neolithic settlements near Osłonki (52°37′N, 18°47′E) in central Poland provide evidence for a mixed economy based on cattle, sheep and goat husbandry, cereal cultivation, fishing and hunting as early as ca. 7300–7200 years ago and definitively during the later period 7000–6000 years ago (Bogucki et al., 2012). The pollen records presented in their study, however, provide little evidence of a dramatic impact on the environment during most of this period and suggest that the area was covered by mixed deciduous and pine forests. The initial appearance of cereal pollen accompanied by continuous but low pollen contents for weeds, pasture indicators, and ruderal plants reflect a low level of agricultural activity. Further east, in the eastern Baltic region and forest zone of European Russia the adoption of Neolithic elements by foragers was very slow and uneven (Zvelebil, 1996, 2008) and started with pottery, continued with livestock and finally cereal cultivation (Bogucki, 2014). Further east, 47 pollen records distributed across the area of Belarus have been interpreted in terms of the initial spread of agriculture (Zernitskaya and Mikhailov, 2009) suggesting the earliest signals of farming (based on discontinuous appearances of *Triticum*, *Hordeum*, and *Secale* pollen types) in the south-western and northern regions at 6600–6000 cal BP and ca. 3400–2700 cal BP, respectively.

Excavated Neolithic sites at Šventoji (56°1′31″N, 21°4′54″E) in Lithuania suggest early agricultural practices in the third millennium BC, though animal and plant domesticates were minor supplements to the hunting-fishing-gathering subsistence (Rimantienė, 1998). Furthermore, a pollen-based reconstruction from Saaremaa Island, Estonia (Poska and Saarse, 2002) – one of the most representative reconstructions of human impact in the eastern Baltic – suggests a replacement of unaffected closed broad-leaved forest by disturbed deciduous forest with first indications of cattle rearing between 6500/6000 and 4500/4200 cal BP and opening of the landscape with restricted cereal cultivation and start of slash-and-burn agriculture between 4500/4200 and 2100/2000 cal BP. However, more intensive cereal cultivation and introduction of rye in the generally open landscape occurred after 2100/2000 cal BP (Poska and Saarse, 2002), in line with our results (Figs. 3–7). The maximum increase in NAP percentages recorded by Poska and Saarse (2002) occurred during the last 1300/1000 years and did not exceed 7–10% of the total pollen sum. Such relatively low NAP values in the peat and lake sediments could be partly explained by overrepresentation of arboreal pollen and underrepresentation of anthropogenic indicators in the samples from agricultural landscapes of northern Europe (Gaillard et al., 1994, 2010; Broström et al., 1998). However, low densities and uneven distribution of population together with a small size of settlements and agricultural fields surrounded by woods should be also considered when interpreting pollen records from lacustrine sediments. On the other hand, pollen analysis of sediment samples collected directly from cultural horizons dated to 4580/4420 and 4090/3870 cal BP demonstrates much higher NAP values (up to 40–60%) and presence of *Cerealia*-type and *Cannabis*-type pollen at the Neolithic and Bronze Age sites near Zvenigorod (55°42′N, 36°43′E), 50–60 km west of Moscow (Ershova et al., 2014, 2016). Suggesting a moderate anthropogenic impact on the forest vegetation at and around the studied archaeological sites, the authors do not exclude the presence of primitive agriculture at the Neolithic sites, but rightly argue for cautious treatment of *Cerealia*-type pollen when discussing the onset of agriculture in the CER region (Ershova et al., 2014). The fact that the *Cerealia*-type pollen group may represent both cultivated and widely distributed wild species of Poaceae has been frequently mentioned (e.g. Beug, 2004; Behre, 2007; Lahtinen and Rowley-Conwy, 2013; Ershova et al., 2014; Demske et al., 2016).

The intensive archaeological excavations provide clear evidence that the mixed forest zone of CER experienced significantly stronger anthropogenic impact during the Iron Age phase (ca. V century BC – V century AD), when numerous walled settlements bonded to river and lake shores spread over the region (Kantorovich, 2006; Mazurkevich et al., 2009; Krenke et al., 2011). Inhabitants of these hill-forts subsisted on animal breeding supplemented by agriculture (e.g. barley, wheat, millet, flax, and hemp), hunting, and fishing. The rich archaeological data (Krenke, 2008, 2011, 2012) from the Moscow region suggest that the Moskva River valley, for example, was well populated since the early Iron Age and that the floodplain landscape, therefore, could have been already heavily transformed at that time. Only the area within the Moscow city borders (ca. 2500 km^2) reveals about 40 hill-fort sites, and a great number of small sites have not been found yet (Krenke, 2012) suggesting a three–four-fold increase in population densities by the V to the III centuries BC. The main occupation period at the best studied hill-fort settlement Djakovo (Krenke, 2011) securely dated to 550 BC to 450 AD shows constant presence of cereal grains through the entire period with the highest concentrations in the layers dated between the I century BC and the II century AD (Krenke et al., 2011). Just before this time interval (i.e. II–I century BC) the shift from bone working to iron implements accompanied with drastic changes in ceramics occurred (Krenke et al., 2011). Similar developmental features including hill-fort settlements (i.e. Podgai, Kovsharovo) and mixed agro-pastoral economy supplemented by traditional hunting and fishing are reported for the western part of the CER mixed forest zone (e.g. Kantorovich, 2006; Mazurkevich et al., 2009). The ‘Dark Ages’ – the period with only scarce archaeological material dating from the VII to the X century AD – suggest a dramatic decrease in population density in the entire region (Krenke, 2012) leading to a quick recovery of the forest vegetation from human pressure. Similar cases of forest regeneration associated with the settlement gap during the Migration Period are well known from the temperate regions of middle Europe (e.g. Litt et al., 2009). Land use across the CER region re-intensified during the early medieval time associated with the spread of Slavic populations. A well-known feature of entire Europe – the increased importance of *Secale* (rye) cultivation since about 1000 years ago (e.g. Litt et al., 2009) – also occurs in the pollen diagrams from CER.

5.2. Palaeoclimatic interpretations and interregional comparison

Since the introduction of pollen analysis into Quaternary research, pollen records have been widely exploited for palaeoclimate reconstructions using a variety of qualitative and quantitative approaches (e.g. Fægri and Iversen, 1989; Berglund and Ralska-Jasiewiczowa, 1986; Birks, 1998). Litt et al. (2009) stressed that reconstructing regional variability of climate change requires detailed comparison and correlation of high resolution palaeoclimatic proxy data with precise chronologies for each record. In the absence of annually laminated lake sediments and high-resolution pollen records with chronological control based on AMS-dated terrestrial plant macrofossils, the CER region is still lacking such high-quality records of palaeoclimate. However, the study area has a great potential for palaeoenvironmental research. In the current chapter the most complete and well-dated century-scale-resolution pollen record of Korovinskoe is used for inter-regional comparison with representative palaeoclimatic records from Europe and the North Atlantic region summarized in Fig. 9.

A noticeable increase in AP percentages in Korovinskoe (Fig. 10A) occurred between ca. 12,000 and 11,500 cal BP in concert with a remarkable increase in temperature (Fig. 10B) evident in the oxygen isotope record from Greenland ice cores (Svensson et al., 2008). This large-scale increase in air temperatures indicating the onset of interglacial environments is echoed in the reconstructions of summer sea surface temperature (SST) derived from diatom (Fig. 10D; Birks and Koç, 2002), mollusk (Fig. 10E; Mangerud and Svendsen, 2018), and foraminifera (Fig. 10F; Hald et al., 2007) records from the Norwegian Sea and western Svalbard. In contrast to the generally synchronous early Holocene temperature increase suggested by various proxies, the onset of the HTM, also called Holocene Thermal Optimum (Houghton et al., 1990), varies between the regions and the records (Davis et al., 2003). In the pollen records from mid-latitude Europe the percentage sum of temperate deciduous tree and shrub taxa (i.e. *Quercetum mixtum*) is frequently used as a terrestrial proxy for reconstructing past thermal conditions. The BIOME vegetation model (Prentice et al., 1992) also demonstrates a strong relationship between the temperate deciduous tree/shrub fraction temperature parameters (i.e. annual sum of growing degree days above 5 °C and mean temperature of the coldest month) in mid-Holocene Europe (Prentice et al., 1996). In the Korovinskoe record (Fig. 10A) the first increase in temperate deciduous tree/shrub percentages is dated to ca. 10,400 cal BP followed by a second, more pronounced increase (up to 21%) between ca. 10,100 and 9800 cal BP. The latter rise corresponds to maximum summer SSTs (i.e. 6–7 °C above the mean modern SST value) reconstructed in the NE North Atlantic (Fig. 10E) and the NW Barents Sea (Fig. 10F). The maximum percentages for temperate deciduous taxa in Korovinskoe (36–46%) are dated to the interval ca. 8600–6900 cal BP corroborating the maximum temperature values in the Greenland ice (Fig. 10B) and the diatom-based August SSTs from the E Norwegian Sea (Fig. 10D). A pollen-based reconstruction of the summer temperature anomaly at Lake Kurjanovas (Fig. 1) in Latvia suggests that the warmest interval in the area located ca. 270 km west of Korovinskoe occurred ca. 8100–5600 cal BP (Fig. 10C; Heikkilä and Seppä, 2010). The registered diachronic patterns of temperature change cannot be explained exclusively by the imperfect age models of the individual records. Mangerud and Svendsen (2018) reported appearance of the most warmth-demanding mollusk species ca. 1000 km farther north of its current distribution indicating that August temperatures on Svalbard were 6 °C warmer at around 10,200–9200 cal BP and that the regional climate was as warm as present by ca. 11,000 cal BP. Furthermore, the authors concluded that exceptionally warm early Holocene climate around Svalbard was driven primarily by higher summer insolation and greater influx of warm Atlantic water, but also influenced by a number of feedback processes including albedo, stronger heating of the shallow water shelf, reduction of sea ice, changes in the atmospheric circulation, etc. Although it is too early for making a solid conclusion, it appears that the final deglaciation of the Scandinavian Ice Sheet (Cuzzone et al., 2016), on the one hand, and the noticeably warmer than present northwestern North Atlantic and western Arctic regions (e.g. Mangerud and Svendsen, 2018), on the other hand, could have been responsible for the earlier onset of warmer conditions in the CER region (Fig. 10A) compared to the eastern Baltic (Fig. 10C), as indicated by the early Holocene spread of the northern tree line in northern Eurasia (e.g. Binney et al., 2009).

Bioclimatic limits estimated for main European tree species (Sykes et al., 1996) and for key regional vegetation types or biomes (Prentice et al., 1996; Kaplan et al., 2003) allow a rough estimation of moisture availability in the study region suggesting that the early Holocene dense forests at Korovinskoe required a moisture index (i.e. the ratio of actual to potential evapotranspiration) above 0.65. The continuous presence of Scots pine in the Holocene forests across CER requires a moisture index above 0.7, while complete disappearance or a negligible presence of spruce in the regional forests prior to ca. 5500 cal BP (Fig. 10G) suggests a decreased moisture availability to below 0.85 (Sykes et al., 1996) during the early Holocene. The presence of spruce macrofossils at 5200 cal BP in the Lake Nero region (Wohlfarth et al., 2006) and a noticeable increase in *Picea* pollen percentages in the Korovinskoe sediments since about 5400 cal BP, with a maximum (ca. 55%) dated to around 2500 cal BP (Fig. 10G), corroborate other published records from the CER region suggesting that spruce survived the relatively dry early and middle Holocene in locally humid habitats (Wohlfarth et al., 2006) and quickly spread across the whole region after the climate conditions became cooler and wetter.

Comparison of modeled and reconstructed changes in climate and forest cover across the middle and northern latitudes of Eurasia through the past 8000 years (Kleinen et al., 2011) suggests that the Holocene trend towards a cooler climate driven by a continuous decrease in summer insolation (Fig. 10I; Berger and Loutre, 1991) was associated with progressively wetter conditions. The reconstructed precipitation derived from the Holzmaar pollen record from the Eifel region in Germany (Fig. 10H; Litt et al., 2009) suggests a relatively moist late Holocene climate in agreement with the model simulation for the mid-latitudinal zone of western Eurasia from Kazakhstan (Kleinen et al., 2011).

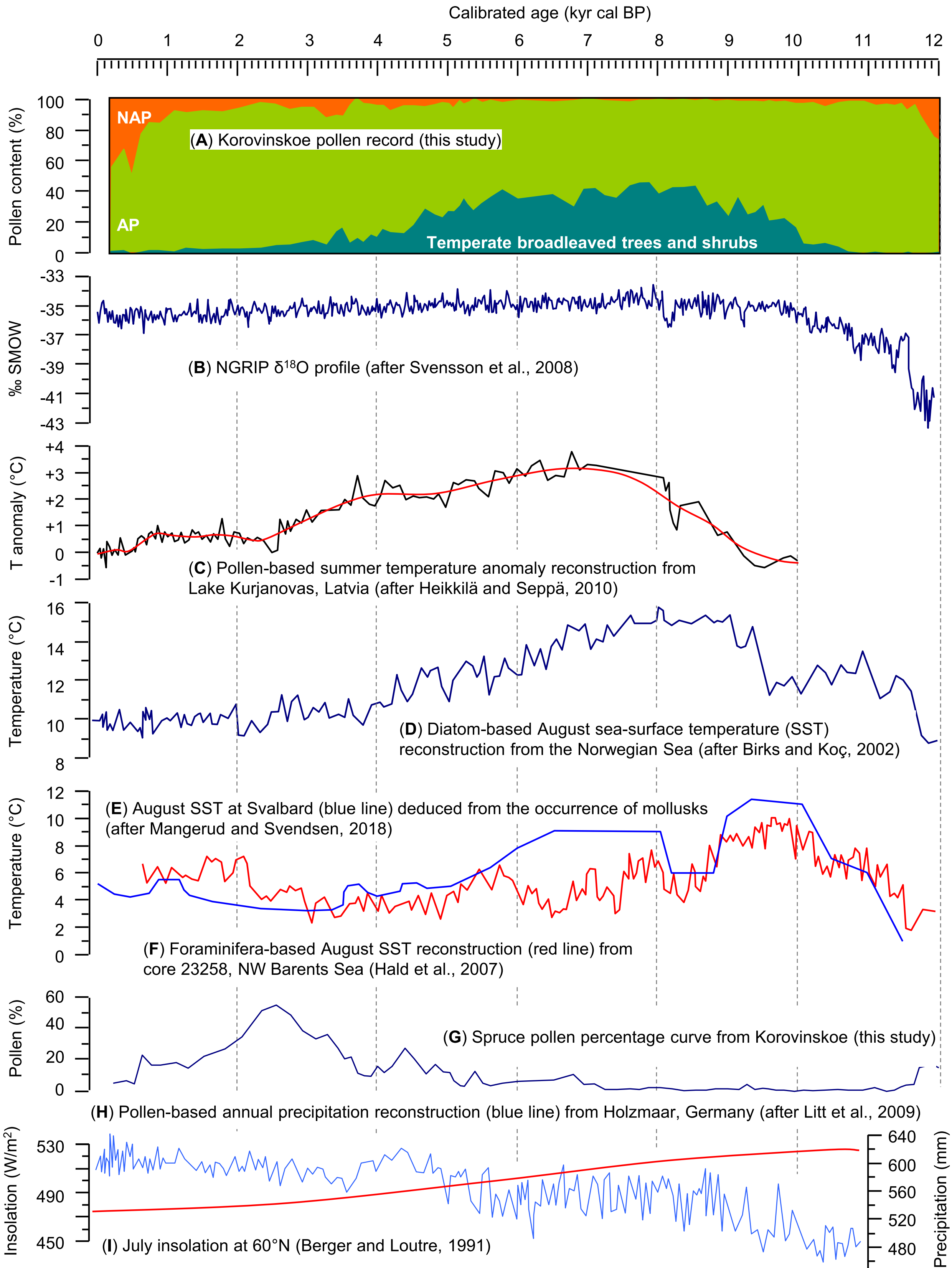

Fig. 10. Comparison of the Korovinskoe pollen record (A) with other palaeoclimate records discussed in the current study (B–I).

6. Conclusions

The current article presents detailed results of palynological investigations obtained for five sediment cores from the upper Western Dvina River located within the cool mixed forest zone of Central European Russia. The cores were extensively dated using a total of 178 bulk sediment samples submitted for conventional radiocarbon dating. Addressing the four key scientific questions formulated in the introduction we came to the following conclusions.

The palynological and radiocarbon dating results suggest that the obtained pollen records cover the entire Holocene at a century-scale resolution. The Lateglacial interval is most likely represented by the Allerød and the Younger Dryas pollen assemblages, however, a more precise discussion of post-glacial vegetation dynamics in the study region requires a better-justified chronology based on AMS dating of terrestrial plant macrofossils. Particularly, the long-year discussion of presence/absence of spruce during the Younger Dryas and the role of woody plants in the Lateglacial vegetation cover cannot be adequately resolved without secure chronological control, which is still unavailable for the entire region.

Checking the synchronicity of the vegetation changes within the study region, we used a pollen-based correlation between the studied records and the regional pollen chronostratigraphy suggested for the CER region by N.A. Khotinsky in the 1970s. Despite its reliance on a few well-studied pollen sequences and an uncalibrated chronology based on a limited number of bulk radiocarbon dates, Khotinsky's scheme became extremely popular and was used by generations of Soviet (later Russian) palynologists for regional and inter-regional correlations facilitating comparisons between poorly dated records. Our study demonstrates straightforward biostratigraphical correlation with the regional Holocene stratigraphy, thus, allowing secure assignment of the local pollen assemblage zones to the Preboreal, Boreal, Atlantic, Subboreal, and Subatlantic periods, and helping in identification of sedimentary hiatuses and possible age reversals in the analyzed records.

Based on the age determinations and pollen-based correlation with the regional biostratigraphy, the Korovinskoe Mire, among the analyzed sequences, was identified as the one with the most complete Holocene sedimentary succession revealing relatively constant sedimentation rates and no apparent reversals or hiatuses. For the first time in the CER region, a Bayesian age modeling approach has been applied to the Korovinskoe dataset in attempt to build a robust calibrated age-depth model for the analyzed pollen record and to allow comprehensive inter-regional comparisons with archaeological and environmental records from elsewhere.

A noticeable increase in woody taxa percentages in Korovinskoe occurred between ca. 12,000 and 11,500 cal BP in concert with a remarkable increase in temperature recorded in Greenland ice cores and in diatom-, mollusk-, and foraminifera-based reconstructions from the North Atlantic. The onset of the so-called 'HTM' in Korovinskoe is reflected by temperate deciduous tree/shrub (*Quercetum mixtum*) pollen percentages. The first pronounced increase (up to 21%) between ca. 10,100 and 9800 cal BP corresponds to the maximum summer SSTs reconstructed for the NE North Atlantic and the NW Barents Sea. The highest *Quercetum mixtum* pollen contents in Korovinskoe (36–46%) are dated to ca. 8600–6900 cal BP, thus corroborating maximum temperature values in Greenland ice and diatom record from the Norwegian Sea, but predating the pollen-derived summer temperature maximum at Lake Kurjanovas (Latvia), which occurred ca. 8100–5600 cal BP. Following some earlier publications, we suggest that the registered diachronic patterns of temperature change cannot be explained exclusively by the imperfect age models of the individual records. They more likely reflect complex interactions of global and regional-scale climate forcing. Primarily the final deglaciation of the Scandinavian Ice Sheet and the noticeably warmer than present northwestern Atlantic and western Arctic regions could have been responsible for the earlier onset of warmer conditions in the CER region compared to the eastern Baltic, as indicated by the early Holocene spread of the northern tree line in northern Eurasia.

A complete disappearance or negligible presence of spruce in the CER forests prior to ca. 5500 cal BP suggests decreased moisture availability during the early Holocene. A noticeable increase in *Picea* pollen percentages in Korovinskoe since about 5400 cal BP, with a maximum (ca. 55%) dated to around 2500 cal BP, corroborates other published pollen and macrofossil records from the CER region, suggesting that spruce survived the relatively dry early and middle Holocene in locally humid habitats and quickly spread across the whole region after the climate conditions became progressively cooler and wetter. This was probably driven by a continuous decline in summer insolation, which led to a decrease in summer temperatures and minimized evaporation losses.

All five pollen records presented in the current study reveal changes, which can be interpreted in terms of growing human impact on the natural forest vegetation and agricultural land use. In contrast to rather synchronous patterns of natural vegetation development, changes which can be assigned to human activities demonstrate substantial spatial/temporal variability. The earliest slight decrease in AP percentages in Korovinskoe, suggesting an initial opening of the pristine forest around the site, occurred about 7700–7600 cal BP. Since then, the pollen spectra demonstrate a more or less continuous decrease in AP contents suggesting further opening of the surrounding landscape, likely associated with human activities. However, a shift towards distinctly lower AP values occurred after 3750 cal BP and a third, even more dramatic, decrease is registered since about 1000 cal BP. First appearance of possible cultivars, such as *Cerealia*-type and *Secale* (rye) pollen, is recorded since ca. 1400 cal BP and during the last millennium, respectively. This pattern of changes may indicate changing human activities and land use close to the site since the Neolithic, starting from the use of wood for construction and making fire by the local sparse hunter-fisher-gatherer population and culminating in the shift to agriculture.

In Prigorodnoe the first appearance of *Secale* accompanied by a slight decreasing trend in the AP curve in Prigorodnoe is dated to 700–600 cal BP. A major drop in AP occurred during the last 500 years. In Serteya 2 the initial decrease in AP percentages coincides with the first appearance of *Trapa natans* and is dated to ca. 5200–5100 cal BP. Pollen grains of *Cerealia*-type and *Secale* are discontinuously present in the record during the last 5000 years, however, in extremely low quantities. In Serteika a continuous decrease in AP percentages is registered between ca. 2600 and 600/700 cal BP and *Cerealia*-type pollen grains are continuously traced during this time interval, becoming more abundant since ca. 1200/1000 cal BP. In Zmeinoe (Fig. 7) the trend towards lower AP values starts ca. 6700 cal BP. At the same time, single pollen grains of *Secale* and *Cerealia*-type appear for the first time in the diagram, though not recorded during the following ca. 5500 years, i.e. until ca. 1200 cal BP. The pollen data does not show a synchronous pattern of changes during the early period of occupation prior to ca. 4000 cal BP suggested by the archaeological records. This can be easily explained by a low density and uneven distribution of prehistoric hunter-fisher-gatherer populations in the densely forested region. However, stepwise strengthening of human impact on the initially dense forest vegetation can be suggested after ca. 4200/3700 cal BP and particularly during the last 1400/1000 years.

Acknowledgements

L. Savelieva and P. Tarasov would like to acknowledge the partnership program of the FU Berlin and St.-Petersburg State University, which facilitated a productive discussion of the data and manuscript writing in St.-Petersburg. The work of T. Long and C. Leipe is financed through the Gerda Henkel Foundation (AZ 06/F/17) and the German Research Foundation (DFG grant LE 3508/1-1), respectively. The authors are grateful to all colleagues and technical assistants who took part in the field work, sample collection, laboratory treatment, and extensive dating of the analyzed sediment cores. The current research contributes to the 'Bridging Eurasia' research initiative supported by the Center for International Cooperation (FU Berlin), the German Archaeological Institute (DAI), and the DFG TA 540/4, TA 540/5 grants to P. Tarasov. The studies carried out at St.-Petersburg State University were supported by the Project No. 18.40.68.2017. Last but not least, careful reading and critical comments done by E. Novenko and two anonymous reviewers helped to improve the manuscript and should be gratefully acknowledged.

References

Alpat'ev, A.M., Arkhangel'skii, A.M., Podoplelov, N.Y., Stepanov, A.Y., 1976. Fizicheskaya Geografiya SSSR (Evropeiskaya Chast'). Vysshaya Shkola, Moscow.
An, C., Ji, D., Chen, F., Dong, G., Wang, H., Dong, W., Zhao, X., 2010. Evolution of prehistoric agriculture in central Gansu province, China: a case study in Qin'an and Li county. Chin. Sci. Bull. 55, 1925–1930.
Andreev, A.A., Tarasov, P.E., 2013. Northern Asia. In: Elias, S.A. (Ed.), The Encyclopedia of Quaternary Science, vol. 4. Elsevier, Amsterdam, pp. 164–172.
Arslanov, KhA., 1993. Late Pleistocene geochronology of European Russia. Radiocarbon 35, 421–427.
Arslanov, KhA., Dolukhanov, P.M., Savelieva, L.A., Dzinoridze, E.N., Kuzmin, G.F., Denisenkov, V.P., 2009. The Holocene environments in north-Western and Central Russia. In: Dolukhanov, P.M., Sarson, G.R., Shukurov, A.M. (Eds.), The East European Plain on the Eve of Agriculture. BAR International Series S1964. Archaeopress Publishers, Oxford, pp. 109–121.
Behre, K.-E., 2007. Evidence for mesolithic agriculture in and around central Europe? Veg. Hist. Archaeobotany 16, 203–219.
Berger, A., Loutre, M.F., 1991. Insolation values for the climate of the last 10 million years. Quat. Sci. Rev. 10, 297–317.
Berglund, B.E., Ralska-Jasiewiczowa, M., 1986. Pollen analysis and pollen diagrams. In: Berglund, B.E. (Ed.), Handbook of Holocene Palaeoecology and Palaeohydrology. John Wiley & Sons, Chichester, New York, pp. 455–484.
Beug, H.-J., 2004. Leitfaden der Pollenbestimmung für Mitteleuropa und angrenzende Gebiete. Verlag Dr. Friedrich Pfeil, München.
Binney, H.A., Willis, K.J., Edwards, M.E., Bhagwat, S.A., Anderson, P., Andreev, A.A., Blaauw, M., Damblon, F., Haesaerts, P., Kienast, F.W., Kremenetski, K.V., Krivonogov, S.K., Lozhkin, A.V., MacDonald, G.M., Novenko, E.Y., Oksanen, P., Sapelko, T.V., Valiranta, M., Vazhenina, L., 2009. The distribution of late-Quaternary woody taxa in northern Eurasia: evidence from a new macrofossil database. Quat. Sci. Rev. 28, 2445–2464.
Birks, H.J.B., 1998. Numerical tools in palaeolimnology – progress, potentialities, and problems. J. Paleolimnol. 20, 307–332.
Birks, C.J.A., Koç, N., 2002. A high-resolution diatom record of late-Quaternary sea-surface temperatures and oceanographic conditions from the eastern Norwegian Sea. Boreas 31, 323–344.
Blaauw, M., Christen, J.A., 2011. Flexible palaeoclimate age-depth models using an autoregressive gamma process. Bayesian Analysis 6, 457–474.
Boaretto, E., Bryant, C., Carmi, I., Cook, G., Gulliksen, S., Harkness, D., Heinemeier, J., McClure, J., McGee, E., Naysmith, P., Possnert, G., Scott, M., van der Plicht, H., Van Strydonck, M., 2002. Summary findings of the fourth international radiocarbon intercomparison (FIRI) (1998-2001). J. Quat. Sci. 17, 633–637.
Bogucki, P., 2014. Hunters, Fishers and farmers of northern Europe 9000-3000 BCE. In: Renfrew, C., Bahn, P. (Eds.), The Cambridge World Prehistory, vol. 3. Cambridge University Press, Cambridge, pp. 1835–1859.
Bogucki, P., Nalepka, D., Grygiel, R., Nowaczyk, B., 2012. Multiproxy environmental archaeology of Neolithic settlements at Osłonki, Poland, 5500–4000 BC. Environ. Archaeol. 17, 45–65.
Bronk Ramsey, C., 1995. Radiocarbon calibration and analysis of stratigraphy: the OxCal program. Radiocarbon 37, 425–430.
Broström, A., Gaillard, M.-J., Ihse, M., Odgaard, B., 1998. Pollen-landscape relationships in modern analogues of ancient cultural landscapes in southern Sweden – a first step towards quantification of vegetation openness in the past. Veg. Hist. Archaeobotany 7, 189–201.
Chairkina, N.M., Kuzmin, Y.V., Hodgins, G.W.L., 2017. Radiocarbon chronology of the mesolithic, neolithic, aeneolithic, and Bronze age sites in the trans-urals (Russia): a general framework. Radiocarbon 59, 505–518.
Cuzzone, J.K., Clark, P.U., Carlson, A.E., Ullman, D.J., Rinterknecht, V.R., Milne, G.A., Lunkka, J.-P., Wohlfarth, B., Marcott, S.A., Caffee, M., 2016. Final deglaciation of the Scandinavian Ice Sheet and implications for the Holocene global sea-level budget. Earth Planet Sci. Lett. 448, 34–41.
d'Alpoim Guedes, J., 2016. Model building, model testing, and the spread of agriculture to the Tibetan Plateau. Archaeological Research in Asia 5, 16–23.
Demske, D., Tarasov, P.E., Leipe, C., Kotlia, B.S., Joshi, L.M., Long, T., 2016. Record of vegetation, climate change, human impact and retting of hemp in Garhwal Himalaya (India) during the past 4600 years. Holocene 26, 1661–1675.
Davis, B.A.S., Brewer, S., Stevenson, A.C., Guiot, J., Contributors, Data, 2003. The temperature of Europe during the Holocene reconstructed from pollen data. Quat. Sci. Rev. 22, 1701–1716.
Dolukhanov, P.M., Shukurov, A., Arslanov, KhA., Mazurkevich, A.N., Savel'eva, L.A., Dzinoridze, E.N., Kulkova, M.A., Zaitseva, G.I., 2004. The Holocene environment and transition to agriculture in boreal Russia (Serteya Valley case study). Internet Archaeol. 17.
Dolukhanov, P.M., Shukurov, A., Gronenborn, D., Timofeev, V.I., Zaitseva, G.I., Sokoloff, D., 2005. The chronology of neolithic dispersal in central and eastern Europe. J. Archaeol. Sci. 32, 1442–1458.
Dolukhanov, P.M., Sarson, G.R., Shukurov, A.M. (Eds.), 2009. The East European Plain on the Eve of Agriculture. BAR International Series S1964. Archaeopress Publishers, Oxford.
Ershova, E.G., Alexandrovskiy, A.L., Krenke, N.A., 2014. Paleosols, paleovegetation and neolithic occupation of the Moskva River floodplain, Central Russia. Quat. Int. 324, 134–145.
Ershova, E.G., Alexandrovskiy, A.L., Krenke, N.A., 2016. Evolution of landscapes of the Moskva River floodplain in the atlantic and subboreal: pedological and palynological records. Catena 137, 611–621.
Fægri, K., Iversen, J., 1989. Textbook of Pollen Analysis. Wiley, Chichester.
Gaillard, M.-J., Birks, H.J.B., Emanuelsson, U., Karlsson, S., Lagerås, P., Olausson, D., 1994. Application of modern pollen/land-use relationships to the interpretation of pollen diagrams – reconstruction of land-use history in south Sweden, 3000–0 BP. Rev. Palaeobot. Palynol. 82, 47–73.
Gaillard, M.-J., Sugita, S., Mazier, F., Trondman, A.-K., Broström, A., Hickler, T., Kaplan, J.O., Kjellström, E., Kokfelt, U., Kuneš, P., Lemmen, C., Miller, P., Olofsson, J., Poska, A., Rundgren, M., Smith, B., Strandberg, G., Fyfe, R., Nielsen, A.B., Alenius, T., Balakauskas, L., Barnekow, L., Birks, H.J.B., Bjune, A., Björkman, L., Giesecke, T., Hjelle, K., Kalnina, L., Kangur, M., van der Knaap, W.O., Koff, T., Lagerås, P., Latałowa, M., Leydet, M., Lechterbeck, J., Lindbladh, M., Odgaard, B., Peglar, S., Segerström, U., von Stedingk, H., Seppä, H., 2010. Holocene land-cover reconstructions for studies on land cover-climate feedbacks. Clim. Past 6, 483–499.
Goring, S., Williams, J.W., Blois, J.L., Jackson, S.T., Paciorek, C.J., Booth, R.K., Marlon, J.R., Blaauw, M., Christen, J.A., 2012. Deposition times in the northeastern United States during the Holocene: establishing valid priors for Bayesian age models. Quat. Sci. Rev. 48, 54–60.
Grichuk, V.P., Zaklinskaya, E.D., 1948. Analiz Iskopaemykh Pyl'tsy I Spor I Ego Primenenie V Paleogeografii. Gosudarstvennoe Izdatel'stvo Geograficheskoi Literatury. Moscow (in Russian).
Grimm, E.C., 1987. CONISS: a FORTRAN 77 program for stratigraphically constrained cluster analysis by the method of incremental sum of squares. Comput. Geosci. 13, 13–35.
Grimm, E.C., 1990. TILIA and TILIA-GRAPH: PC Speadsheet and Graphics Software for Pollen Data. INQUA Working Group on Data-Handling Methods Newsletter 4, pp. 5–7.
Grimm, E.C., 2000. TGView and Tilia for Windows. INQUA Sub-Commission on Data-Handling Methods Newsletter 20, p. 5.
Gunova, V.S., Tarasov, P.E., Uspenskaya, O.N., Pushenko, M.Ya, MacDonald, G.M., 2001. Holocene evolution of the trostenskoe lake and adjacent area. *Vestnik-Moskovskogo universiteta* Ser. 5. Geography 1, 61–67 (in Russian).
Hald, M., Andersson, C., Ebbesen, H., 2007. Variations in temperature and extent of Atlantic Water in the northern North Atlantic during the Holocene. Quat. Sci. Rev. 26, 3423–3440.
Heikkilä, M., Seppä, H., 2010. Holocene climate dynamics in Latvia, eastern Baltic region: a pollen-based summer temperature reconstruction and regional comparison. Boreas 39, 705–719.
Houghton, J.T., Jenkins, G.J., Ephraums, J.J. (Eds.), 1990. Climate Change: the IPCC Scientific Assessment. Cambridge University Press, Cambridge, UK.
Hua, Q., Barbetti, M., Rakowski, A.Z., 2013. Atmospheric radiocarbon for the period 1950–2010. Radiocarbon 55, 2059–2072.
Jones, G., Jones, H., Charles, M.P., Jones, M.K., Colledge, S., Leigh, F.J., Lister, D.A., Smith, L.M.J., Powell, W., Brown, T.A., 2012. Phylogeographic analysis of barley DNA as evidence for the spread of Neolithic agriculture through Europe. J. Archaeol. Sci. 39, 3230–3238.
Kantorovich, A.R., 2006. Rannii zheleznyi vek v lesostepnoi i lesnoi zonakh Vostochnoi Evropy. In: Yanin, V.L. (Ed.), Archeologiya. MGU, Moscow, pp. 360–370 (in Russian).
Kaplan, J.O., Bigelow, N.H., Prentice, I.C., Harrison, S.P., Bartlein, P.J., Christensen, T.R., Cramer, W., Matveyeva, N.V., McGuire, A.D., Murray, D.F., Razzhivin, V.Y., Smith, B., Walker, D.A., Anderson, P.M., Andreev, A.A., Brubaker, L.B., Edwards, M.E., Lozhkin, A.V., 2003. Climate change and Arctic ecosystems: 2. Modeling, paleodata-model comparisons, and future projections. J. Geophys. Res. 108 (8171), 17. https://doi.org/10.1029/2002JD002559.
Königsson, L.K., Possnert, G., 1997. Pollen analysis covering the past 4000 radiocarbon years of cultural landscape of the Novgorod area, Russia. Birka Studies 4.

Environment and Vikings: scientific methods and techniques. ISSN 91-7209-067-7, 52, 73–89.
Khotinsky, N.A., 1977. Holocene of the Northern Eurasia. Nauka, Moscow (in Russian with English Abstract).
Khotinsky, N.A., 1980. Tri tipa izmeneniya klimata Severnoi Evrazii v golotsene (Three types of climate change in the Holocene of Northern Eurasia). In: Adrianov, B.V., Zorin, L.V., Nikolaeva, R.V. (Eds.), Kolebaniya Uvlazhnennosti Aralo-kaspiiskogo Regiona v Golotsene. Nauka, Moscow, pp. 5–11 (in Russian).
Khotinsky, N.A., Klimanov, V.A., 1997. Allerød, younger Dryas and early Holocene palaeoenvironmental stratigraphy. Quat. Int. 41/42, 67–70.
Klimanov, V.A., 1984. Palaeoclimatic reconstructions based on the information-statistical method. In: Velichko, A.A. (Ed.), Late Quaternary Environments of the Soviet Union. University of Minnesota Press, Minneapolis, pp. 297–304.
Kleinen, T., Tarasov, P., Brovkin, V., Andreev, A., Stebich, M., 2011. Comparison of modeled and reconstructed changes in forest cover through the past 8000 years: Eurasian perspective. Holocene 21, 723–734.
Krementski, K.V., Borisova, O.K., Zelikson, E.M., 2000. The late glacial and Holocene history of vegetation in the Moscow region. Paleontol. J. 34, 67–74 in Russian.
Krenke, N.A., 2008. Formation of the cultural landscape in the Moscow river basin from the Bronze age to medieval times. Anthropol. Archeol. Eurasia 47 (1), 57–81.
Krenke, N.A., 2011. Dyakovo Hillfort: the Culture of the Population of the Moskva Basin in the 1st Millennium BC – 1st Millenium AD. Institut Arkheologii RAN, Moscow in Russian with English Abstract.
Krenke, N.A., 2012. The Moskva River basin in the iron age – Migration Period. Archaeologia Baltica 17, 91–100.
Krenke, N.A., Aleksandrovsky, A.L., Lazurkin, A.V., Spiridonova, E.A., 2011. Farmers and cattle breeders of Bronze and iron ages at Moscow river banks: new discoveries. Vestnik rossiiskogo fonda fundamentalnykh issledovanii. Gumanitarnye i obshchestvennye nauki 3 (64), 147–158.
Lahtinen, M., Rowley-Conwy, P., 2013. Early farming in Finland: was there cultivation before the iron age (500 BC)? Eur. J. Archaeol. 10, 1–25.
Litt, T., Stebich, M., 1999. Bio- and chronostratigraphy of the lateglacial in the Eifel region. Germany. Quaternary International 61, 5–16.
Litt, T., Schölzel, C., Kühl, N., Brauer, A., 2009. Vegetation and climate history in the Westeifel Volcanic Field (Germany) during the past 11000 years based on annually laminated lacustrine maar sediments. Boreas 38, 679–690.
Ma, T., Tarasov, P.E., Zheng, Z., Han, A., Huang, K., 2016. Pollen- and charcoal-based evidence for climatic and human impact on vegetation in the northern edge of Wuyi Mountains, China, during the last 8200 years. Holocene 26, 1616–1626.
Mangerud, J., Svendsen, J.I., 2018. The Holocene Thermal Maximum around Svalbard, arctic North Atlantic; mollusks show early and exceptional warmth. Holocene 28, 65–83..
Mazurkevich, A.N., Korotkevich, B.N., Dolukhanov, P.M., Shukurov, A.M., Arslanov, KhA., Savel'eva, L.A., Dzinoridze, E.N., Kulkova, M.A., Zaitseva, G.I., 2009. Climate, subsistence and human movements in the western Dvina – Lovat river basins. Quat. Int. 203, 52–66.
Mazurkevich, A., Kulkova, M., Savel'eva, L., 2012. Chapter 2.2. Human occupation history of the upper Dvina basin. In: Geoarchaeological Issues of the Upper Dnieper –Western Dvina River Region (Western Russia): Fieldtrip Guide. Universum, Moscow-Smolensk, pp. 70–104.
Miklyaev, A.M., 1995. Kamennyi-zheleznyi vek v mezhdurech'e Zapadnoi Dviny i Lovati. Peterburgskii Arheologicheskii Vestnik 9, 7–39.
Muraki, Y., Masuda, K., Arslanov, K.A., Toyoizumi, H., Kato, M., Naruse, Y., Murata, T., Nishiyama, T., 2001. Measurement of radiocarbon content in leaves from some Japanese sites. Radiocarbon 43, 695–701.
Neishtadt, M.I., 1957. Istoriya Lesov I Paleogeografiya SSSR V Golotsene (History of Forests and Palaeogeography of the USSR in the Holocene Period). Izdatel'stvo Akademii Nauk SSSR. Moscow (in Russian).
Novenko, E.Yu, Olchev, A.V., 2015. Early Holocene vegetation and climate dynamics in the central part of the East European Plain (Russia). Quat. Int. 388, 12–22.
Novenko, E.Yu, Volkova, E.M., Nosova, N.B., Zuganova, I.S., 2009. Late glacial and Holocene landscape dynamics in the southern taiga zone of East European plain according to pollen and macrofossil records from the central forest state reserve (Valdai hills, Russia). Quat. Int. 207, 93–103.
Novenko, E.Y., Tsyganov, A.N., Volkova, E.M., Babeshko, K.V., Lavrentiev, N.V., Payne, R.J., Mazei, Y.A., 2015. The Holocene paleoenvironmental history of central European Russia reconstructed from pollen, plant macrofossil, and testate amoeba analyses of the Klukva peatland, Tula region. Quat. Res. 83, 459–468.
Payne, R.J., Malysheva, E., Tsyganov, A., Pampura, T., Novenko, E., Volkova, E., Babeshko, K., Mazei, Y., 2016. A multi-proxy record of Holocene environmental change, peatland development and carbon accumulation from Staroselsky Moch peatland, Russia. Holocene 26, 314–326.
Prentice, I.C., Cramer, W., Harrison, S.P., Leemans, R., Monserud, R.A., Solomon, A.M., 1992. A global biome model based on plant physiology and dominance, soil properties and climate. J. Biogeogr. 19, 117–134.
Prentice, I.C., Guiot, J., Huntley, B., Jolly, D., Cheddadi, R., 1996. Reconstructing biomes from palaeoecological data: a general method and its application to European pollen data at 0 and 6 ka. Clim. Dynam. 12, 185–194.
Poska, A., Saarse, L., 2002. Vegetation development and introduction of agriculture to Saaremaa Island, Estonia: the human response to shore displacement. Holocene 12, 555–568.
R Core Team, 2016. R: a Language and Environment for Statistical Computing. R Foundation for Statistical Computing. Vienna.
Reimer, P.J., Bard, E., Bayliss, A., Beck, J.W., Blackwell, P.G., Bronk Ramsey, C., Buck, C.E., Cheng, H., Edwards, R.L., Friedrich, M., Grootes, P.M., Guilderson, T.P., Haflidason, H., Hajdas, I., Hatté, C., Heaton, T.J., Hoffmann, D.L., Hogg, A.G., Hughen, K.A., Kaiser, K.F., Kromer, B., Manning, S.W., Niu, M., Reimer, R.W., Richards, D.A., Scott, E.M., Southon, J.R., Staff, R.A., Turney, C.S.M., van der Plicht, J., 2013. IntCal13 and MARINE13 radiocarbon age calibration curves 0–50,000 years cal BP. Radiocarbon 55, 1869–1887.
Reimer, P.J., Brown, T.A., Reimer, R.W., 2004. Discussion: reporting and calibration of post-bomb 14C data. Radiocarbon 46, 1299–1304.
Rimantienė, R., 1998. The first Narva Culture farmers in Lithuania. In: Zvelebil, M., Domańska, L., Dennell, R. (Eds.), Harvesting the sea, farming the forest: The emergence of Neolithic societies inthe Baltic Region. Sheffield Academic Press, Sheffield, pp. 213–218.
Slobodin, V.M., 1952. K voprosu o razvitii i smene sistem zemledeliya. In: Grekov, B.D. (Ed.), Materialy Po Istorii Zemledeliya SSSR. Izdatel'stvo Akademii Nauk SSSR, Moscow, pp. 9–65 (in Russian).
Smith, B.D., 2001. Low-level food production. J. Archaeol. Res. 9 (1), 1–43.
Spengler, R.N., Ryabogina, N., Tarasov, P.E., Wagner, M., 2016. The spread of agriculture into northern Central Asia: timing, pathways, and environmental feedbacks. Holocene 26, 1527–1540.
Svensson, A., Andersen, K.K., Bigler, M., Clausen, H.B., Dahl-Jensen, D., Davies, S.M., Johnsen, S.J., Muscheler, R., Parrenin, F., Rasmussen, S.O., Rothlisberger, R., Seierstad, I., Steffensen, J.P., Vinther, B.M., 2008. A 60 000 year Greenland stratigraphic ice core chronology. Clim. Past 4, 47–57.
Sykes, M.T., Prentice, I.C., Cramer, W., 1996. A bioclimatic model for the potential distributions of north European tree species under present and future climates. J. Biogeogr. 23, 203–233.
Velichko, A.A., Andreev, A.A., Klimanov, V.A., 1997. Climate and vegetation dynamics in the tundra and forest zone during the Late Glacial and Holocene. Quat. Int. 41/42, 71–96.
Veski, S., Amon, L., Heinsalu, A., Reitalu, T., Saarse, L., Stivrins, N., Vassiljev, J., 2012. Lateglacial vegetation dynamics in the eastern Baltic region between 14,500 and 11,400 cal yr BP: a complete record since the Bølling (GI-1e) to the Holocene. Quat. Sci. Rev. 40, 39–53.
Weather and climate, 2016. http://www.pogodaiklimat.ru/climate/26781.htm, accessed on 08.09.2016.
Wohlfarth, B., Tarasov, P., Bennike, O., Lacourse, T., Subetto, D., Torssander, P., Romanenko, F., 2006. Late glacial and Holocene palaeoenvironmental changes in the Rostov-Yaroslavl' area, West Central Russia. J. Paleolimnol. 35, 543–569.
Wohlfarth, B., Lacourse, T., Bennike, O., Subetto, D., Tarasov, P., Demidov, I., Filimonova, L., Sapelko, T., 2007. Climatic and environmental changes in north-western Russia between 15,000 and 8000 cal yr BP: a review. Quat. Sci. Rev. 26, 1871–1883.
Zhao, L., Ma, C., Leipe, C., Long, T., Liu, K., Lu, H., Tang, L., Zhang, Y., Wagner, M., Tarasov, P.E., 2017. Holocene vegetation dynamics in response to climate change and human activities derived from pollen and charcoal records from south-eastern China. Palaeogeography, Palaeoclimatology. Palaeoecology 485, 644–660.
Zernitskaya, V., Mikhailov, N., 2009. Evidence of early farming in the Holocene pollen spectra of Belarus. Quat. Int. 203, 91–104.
Zvelebil, M., 1996. The agricultural frontier and transition to farming in the circular-Baltic region. In: Harris, D.R. (Ed.), The Origins and Spread of Agriculture and Pastoralism in Eurasia. UCL Press, London, pp. 323–345.
Zvelebil, M., 2008. Innovating hunter-gatherers: the mesolithic in the baltic. In: Nailey, G., Spikins, P. (Eds.), Mesolithic Europe. Cambridge University Press, Cambridge, pp. 18–59.